Available online at www.sciencedirect.com
ScienceDirect
Biochemical and Biophysical Research Communications 365 (2008) 279–284
BBRC
www.elsevier.com/locate/ybbrc

Mutant MCP-1 therapy inhibits tumor angiogenesis and growth of malignant melanoma in mice

Mitsuhisa Koga [a], Hisashi Kai [a,*], Kimiyasu Egami [b], Toyoaki Murohara [d], Ayami Ikeda [a], Suguru Yasuoka [a], Kensuke Egashira [e], Toyojiro Matsuishi [b], Mamiko Kai [f], Yasufumi Kataoka [g], Michihiko Kuwano [c], Tsutomu Imaizumi [a]

[a] *Department of Internal Medicine, Division of Cardio-Vascular Medicine and Cardiovascular Research Institute, Kurume University School of Medicine, 67 Asahimachi, Kurume 830-0011, Japan*
[b] *Department of Pediatrics, Kurume University School of Medicine, Kurume, Japan*
[c] *Research Center for Innovative Cancer Therapy, Kurume University School of Medicine, Kurume, Japan*
[d] *Department of Cardiology, Nagoya University Graduate School of Medicine, Nagoya, Japan*
[e] *Department of Cardiovascular Medicine, Kyushu University Graduate School of Medicine, Fukuoka, Japan*
[f] *Department of Pharmaceutics, Inenaga Hospital, Chikuzen, Japan*
[g] *Department of Pharmaceutical Care and Health Sciences, Faculty of Pharmaceutical Sciences, Fukuoka University, Fukuoka, Japan*

Received 19 October 2007
Available online 6 November 2007

Abstract

We investigated whether blocking of monocyte chemoattractant-1 (MCP-1) function would inhibit recruitment of tumor-associated macrophages (TAMs) and prevent tumor angiogenesis and tumor growth of human malignant melanoma. B16-F1 melanoma cells were implanted onto the back of C57BL/6 mice (Day 0). At Day 7, a dominant negative MCP-1 mutant (7ND) gene was transfected in the thigh muscle to make overexpressed 7ND protein secreted into systemic circulation. 7ND treatment inhibited TAM recruitment and partially reduced tumor angiogenesis and tumor growth. Also, 7ND treatment attenuated inductions of tumor necrosis factor-α (TNFα), interleukin-1α (IL-1α), and vascular endothelial growth factor (VEGF) in the stroma and tumor. Melanoma cells expressed not only MCP-1 but also its receptor CCR2. Accordingly, it was suggested that MCP-1 would enhance tumor angiogenesis and early tumor growth in the early stages by inducing TNFα, IL-1α, and VEGF through TAM recruitment and probably the direct autocrine/paracrine effects on melanoma cells.

Keywords: MCP-1; Macrophages; Melanoma; Angiogenesis; Inflammation; Gene therapy; Cytokines; VEGF

There is increasing evidence that recruitment of tumor-associated macrophages (TAMs) in the stroma, and loose connective tissue surrounding the tumor is an important trigger for tumor angiogenesis [1], which promotes tumor growth and hematogeneous metastases [2–5]. The stromal TAM recruitment is related to poor prognosis of human cancers [6–11]. Monocyte chemoattractant protein-1 (MCP-1) is a potent macrophage-recruiting molecule. It was reported that MCP-1 was expressed during the early stages of human malignant melanoma [12,13]. However, it has remained unknown whether MCP-1 production has causal relationships with TAM recruitment, tumor angiogenesis, and early tumor growth of malignant melanoma.

A mutant of MCP-1, which lacks the N-terminal amino acids 2–8 (7ND), has a potent dominant negative activity [14]. We have shown that transduction of 7ND gene in

Abbreviations: MCP-1, monocyte chemoattractant protein-1; 7ND, a dominant negative MCP-1 mutant lacking the N-terminal amino acids 2–8; TAM, tumor-associated macrophage; VEGF, vascular endothelial growth factor; IL-1α, interleukin-1α; TNFα, tumor necrosis factor-α; PCR, recombinant polymerase chain reaction; RT-PCR, reverse-transcribed PCR.

* Corresponding author. Fax: +81 942 33 6509.
E-mail address: naikai@med.kurume-u.ac.jp (H. Kai).

0006-291X/$ - see front matter © 2007 Elsevier Inc. All rights reserved.
doi:10.1016/j.bbrc.2007.10.182

the thigh muscle as means to make overexpressed 7ND protein secreted into systemic circulation is a useful strategy for blocking MCP-1 activity in the remote target organs, such as atherosclerotic artery and heart [15,16]. Moreover, we have demonstrated that 7ND overexpression inhibits ischemia-induced neovascularization in the mouse hindlimb by preventing macrophage recruitment and vascular endothelial growth factor (VEGF) production [17]. In the present study, we sought to determine blocking of intrinsic MCP-1 by 7ND treatment would inhibit the initiation of tumor angiogenesis and early growth of human malignant melanoma engrafted in mice.

Materials and methods

The present study protocol was reviewed and approved by the Animal Care and Treatment Committee of Kurume University. Male C57BL/6 mice were purchased from Clea Japan Inc. (Tokyo, Japan) and housed under standard conditions of humidity, room temperature, and dark–light cycles in plenty of chow and water.

Expression vector. Human 7ND cDNA was constructed by recombinant polymerase chain reaction (PCR) using a wild type MCP-1 cDNA and cloned into BamHI (5′) and NotI (3′) sites of the pCDNA3 expression plasmid vector (Invitrogen Corp., Tokyo) [15]. The dominant negative activity was verified in vivo as described previously [15].

Tumor-implanted mouse model. We employed B16-F1 melanoma cells (Batch No. 1224725, Flask Passage No. 26; American Type Culture Collection, Manassas, VA), which can grow in the C57BL/6 strain [18] for a mouse model of tumor angiogenesis [18,19]. B16-F1 melanoma cells were cultured in DMEM supplemented with 4 mmol/L of L-glutamine, 2.5 g/L glucose, 10% fetal bovine albumin, and antibiotics and were harvested as described previously [19]. Under anesthesia with intraperitoneal pentobarbital (30 mg/kg), 1×106 B16-F1 melanoma cells were solved in 200 μL of phosphate-buffered saline (PBS) and injected subcutaneously into the back of C57BL/6 mice at 8-week old (Day 0).

7ND gene transfer. Naked cDNA method was used for 7ND gene transfer, as described previously [17,20]. Briefly, at Day 4, bupivacaine (12.5 μg/g body weight; AstraZeneka, Tokyo) was injected into the thigh muscle to improve the efficiency of gene transfer [21]. At Day 7, 7ND plasmid or the blank plasmid (control) solved in 30 μL PBS was injected at the same site as bupivacaine had been injected. We confirmed preliminary that a single 7ND gene transfer elevated serum 7ND protein levels at least for 14 days after gene transfer, and that 200 μg was the minimum dose that induced the maximum serum level elevation and did not cause histological damage of the thigh muscle at the site of gene transfer [17]. Thus, 200 μg of 7ND plasmid was injected throughout the following experiments.

Tumor volume measurement. Tumor size was measured using a caliper at denoted days ($n = 9$/group). Tumor volume was calculated according to the formula: tumor volume (mm^3) $= (L \times W^2) \times 0.52$, where L = length (mm) and W = width (mm) (length is greater than width) [22].

Tumor microangiography. Postmortem tumor microangiography was performed using an X-ray mammography system (Senographe 500T; GE Medical Systems-Europe, Paris) at Day 13 [19].

Immunohistochemical analysis of capillary density and TAM infiltration. At Day 13, mice were euthanized by an overdose pentobarbital. Tumor and the stroma (surrounding subcutaneous tissue approximately 3 mm from the tumor margin) were carefully isolated, fixed in methanol overnight, embedded in paraffin, and sectioned into 5-μm slices [19]. The sections ($n = 5$/group) were subjected to immunohistochemistry using monoclonal antibodies against mouse MCP-1 (SantaCruz Biotechnology, Santa Cruz, CA), mouse CCR2 (SantaCruz Biotechnology), mouse CD31 (PharMingen, San Diego, CA), mouse F4/80 (Serotec, Raleigh, CA), and a commercially available detection kit (Dako, Glosup, Denmark) [23].

The capillary was defined as the luminal structure surrounded by CD31-labeled endothelial cells (ECs) [19]. The number of the capillaries and F4/80-labeled macrophages was counted and averaged in 15 random microscopic fields of the tumor and stroma from 3 independent sections in each animal. Necrotic cores inside the tumor were excluded from the analysis. Capillary density and TAM count were expressed as the number of capillaries and macrophages per high-power field (400×), respectively.

RT-PCR analysis. At Day 13, after mice were euthanized with an overdose of pentobarbital and perfused with ice-cold PBS, the tumor and stroma were excised en bloc ($n = 5$/group). The tumor was carefully resected from the stroma. Total RNA was extracted from the tumor and stroma using TRIzol reagent (Invitrogen) and reverse-transcribed by using Ready-To-Go You-Prime First-Strand Beads (Amersham, NJ, USA) [24]. Equal amount of the resulting cDNA was subjected to PCR with a primer pair and a Taq DNA polymerase kit (Toyobo, Tokyo, Japan), according to the manufacturer's instructions. The nucleotide sequences of primers were as follows: for VEGF (sense) 5′-GCC AGC ACA TAG AGA GAA TGA GC-3′ and (antisense) 5′-CAA GGC TCA CAG TGA TTT TCT GG-3′; for IL-1α (sense) 5′-CGT CAG GCA GAA GTT TGT CA-3′ and (antisense) 5′-GTG CAC CCG ACT TTG TTC TT-3′; and for TNFα (sense) 5′-ACG GCA TGG ATC TCA AAG AC-3′ and (antisense) 5′-CGG ACT CCG CAA AGT CTA AG-3′. Primer pairs for MCP-1, CCR2, and GAPDH were purchased from Proligo (Tokyo, Japan). Cycle numbers of amplification were 32 cycles for MCP-1, CCR2, VEGF, IL-1α, and TNFα and 25 cycles for GAPDH (95 °C for 1 min, 60 °C for 1 min, and 72 °C for 45 s). The PCR products were separated on 1.5% agarose gel stained with ethidium bromide. The signals were scanned and analyzed with digital densitometry. The expression level of target gene was normalized for the GAPDH level in each sample [25].

Statistics. Data are means ± SE. Unpaired Student's t test was performed for statistical comparison. A p value less than 0.05 was considered statistically significant.

Results and discussion

Early tumor growth, TAM infiltration, and tumor angiogenesis

At Day 7, implanted B16-F1 melanoma cells began to be seen as grossly visible tumor (Fig. 1), although F4/80-positive macrophages, TAMs, and tumor-related angiogenesis were not observed in the stroma (data not shown). To determine the effects of MCP-1 function blocking on TAM recruitment and the initiation of tumor angiogenesis, 7ND gene transfer was performed into the thigh muscle at Day 7.

In control mice, tumor enlarged progressively after Day 7 and huge tumor developed at Day 13 (Fig. 1). Postmortem tumor microangiography showed the formation of tumor-feeding vessels (Fig. 2A). Control mice showed a lot of CD31-labeled capillary vessels with various luminal sizes in the stroma, whereas the inside of the tumor was rich in small-sized capillaries (Fig. 2B). At Day 13, diffuse TAM infiltration was observed in the stroma, whereas TAMs were scarcely found inside the tumor (Fig. 2C).

When mice received 7ND treatment, the tumor volume was significantly reduced until Day 13 (Fig. 1). The formation of angiographically visible tumor-related vessels was reduced by 7ND treatment (Fig. 2A). 7ND treatment reduced the tumor-related capillary density in the stroma and tumor by 33% and 23%, respectively (Fig. 2B). Moreover, 7ND treatment reduced TAM recruitment by 50% in the TAM number (Fig. 2C).

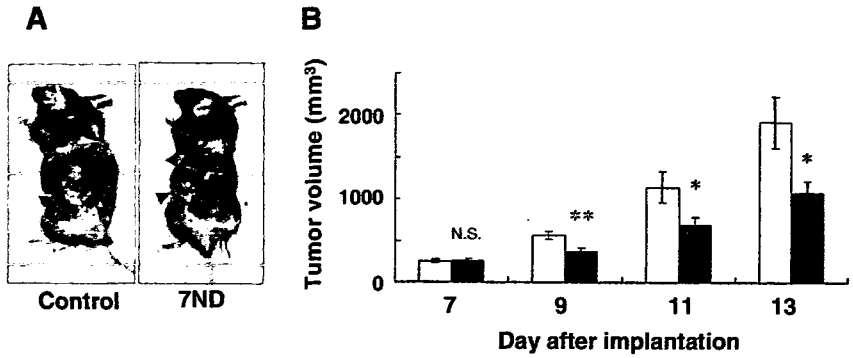

Fig. 1. (A) Representative photographs of engrafted tumors at Day 13 after B16-F1 melanoma cells implantation. (B) Time course of tumor volume. 7ND-treated mice (closed column) received 7ND gene transfer into the thigh muscle at Day 7. Control mice (open column) received the blank plasmid injection. Bar = 1 × SM ($n = 9$). $^{*}p < 0.05$ and $^{**}p < 0.01$ vs. control.

The present study suggests that MCP-1 not only acts as the TAM-recruiting molecules but also promotes the initiation of tumor angiogenesis and early tumor growth of malignant melanoma. Earlier studies demonstrated that the stromal TAMs trigger tumor angiogenesis [1]. Because nutritional tumor angiogenesis is crucial for tumor growth [2–5], our results suggest that MCP-1-mediated TAM recruitment might enhance the early growth of malignant melanoma by increasing tumor angiogenesis.

MCP-1 and CCR2 expression

In control mice at Day 13, most of malignant melanoma cells expressed immunoreactive MCP-1 (Fig. 3A), consistent with earlier studies [12,13]. It was noteworthy that CCR2, the sole receptor for MCP-1, was expressed in the majority of malignant melanoma cells as well. To our best knowledge, this is the first report that malignant melanoma cells express not only MCP-1 but also its receptor. 7ND treatment reduced the melanoma cells expressing MCP-1 and CCR2 (Fig. 3B). This finding may suggest that MCP-1 creates positive feedback loop for activating melanoma cells in an autocrine/paracrine manner. Also, a part of the stromal TAMs expressed MCP-1 and CCR2 and they were reduced by 7ND treatment.

Angiogenic factor and inflammatory cytokine expressions

VEGF is a major angiogenic factor and is produced by melanoma cells and TAMs in this model [19]. A recent in vitro study has shown that activated macrophages produce IL-1α and TNFα, which in turn induce VEGF production of cultured melanoma cells [1]. Moreover, TAMs have been shown to be prerequisite for neovascularization and tumor growth of Lewis lung cancer cells in the cornea model [26]. Thus, we examined the effects of 7ND treatment on the expressions of IL-1α, TNFα, and VEGF (Fig. 4). It is noteworthy that IL-1α and TNFα inductions were potent in not only the stroma but also the tumor in this model. The most important, novel finding of this study is that 7ND treatment remarkably reduced inductions of the inflammatory cytokines and VEGF in the tumor and stroma. Since TAM number was small and was not changed by 7ND treatment (Fig. 2C), the changes in cytokine and VEGF expressions in the tumor were attributable to melanoma cells. In addition to TAM recruitment, MCP-1 may directly activate VEGF induction and proliferation of malignant melanoma cells via the CCR2 activation in autocrine/paracrine fashion (Fig. 3). Moreover, MCP-1 would enhance tumor growth at least in part through the direct effects of IL-1α and TNFα on malignant melanoma cells. Recent studies have shown that IL-1α promotes tumor growth by directly enhancing melanoma cell proliferation and by activating inflammatory and angiogenic pathway in the stroma [27] and that TNFα prolongs tumor cell survival through the anti-apoptotic effect [28]. Taken together, MCP-1 may induce tumor angiogenesis and early tumor growth of human malignant melanoma by inducing VEGF and inflammatory cytokines through the TAM recruitment and the direct autocrine/paracrine effects on melanoma cells. Recently, it has been demonstrated that inflammatory stimuli from TAMs and tumor cells synergistically promote tumor growth and angiogenesis [29]. From the present study, however, we were not able to determine the precise interaction of these cytokines and VEGF. This issue should be addressed in future study.

There are several limitations in this study. First, the inhibitions of TAM recruitment, tumor angiogenesis, and early tumor growth by 7ND treatment were partial in this study. If higher local concentration of 7ND could be achieved, we might have more potent effects. Second, from this study, we did not know the long-term effects on tumor growth and prognosis. To address these issues, the improvement of the expression efficiency (i.e. the adjunctive treatment for naked DNA method or the use of viral expression vectors) and/or repeated gene transfers would be necessary for sustained transgene expression at higher level for longer periods. Finally, we do not deny the possibility of the involvement of direct angiogenic effect of MCP-1 on the ECs via the CCR2 activation [30].

In conclusion, MCP-1 may play a role in tumor angiogenesis and early tumor growth of human malignant mela-

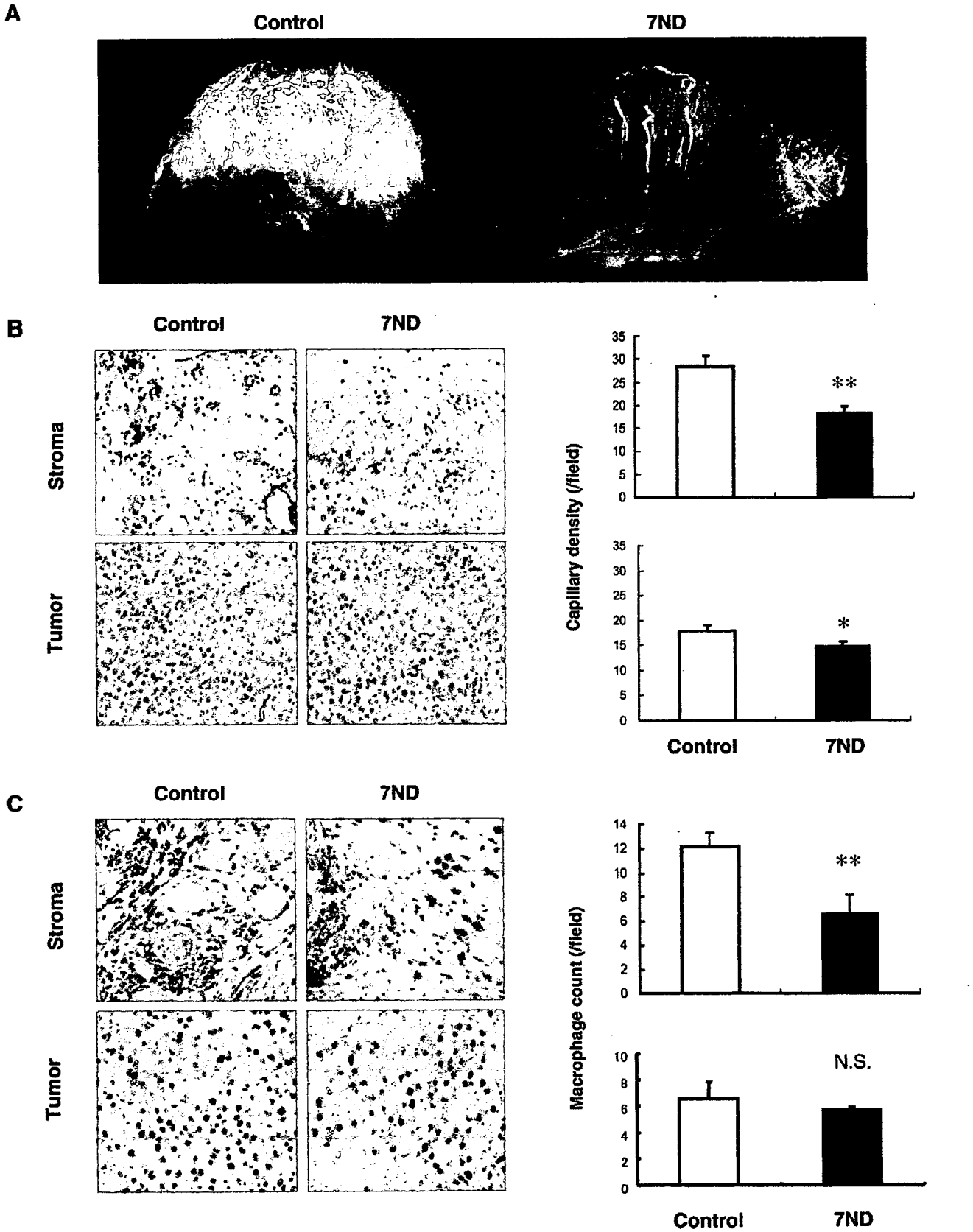

Fig. 2. (A) Representative tumor microangiograms of control and 7ND-treated mice at Day 13. Representative immunohistostainings (left) and the pooled data (right) showing effects of 7ND treatment on the capillary density (B) and TAM infiltration (C) at Day 13. Bar = 1 × SM ($n = 5$). $^{*}p < 0.05$ and $^{**}p < 0.01$ vs. control.

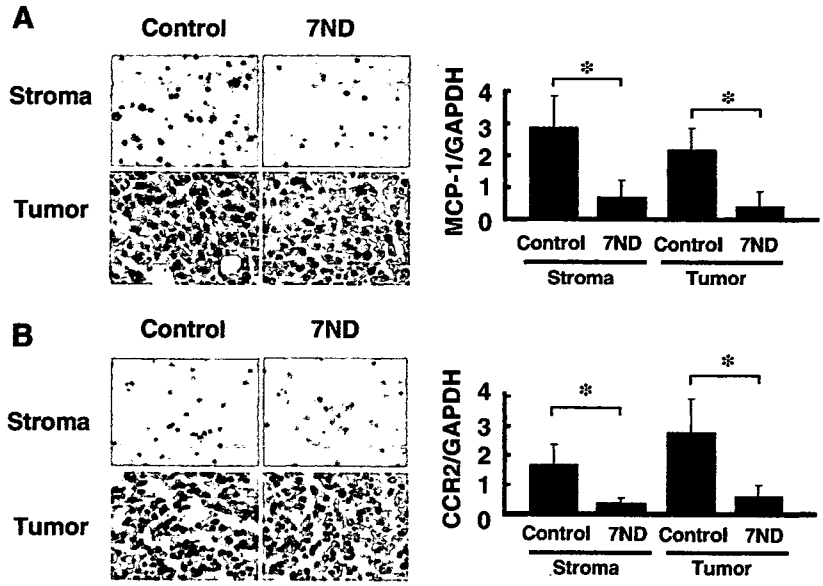

Fig. 3. Representative immunohistostainings (left) and the pooled data (right) of mRNA expression of MCP-1 (A) and CCR2 (B) at Day 13. Bar = 1 × SM ($n = 5$). $^{*}p < 0.05$ vs. control.

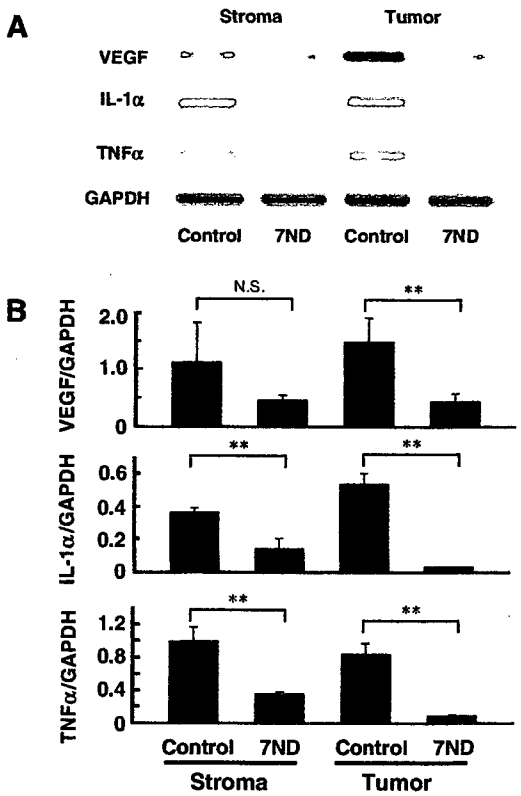

Fig. 4. (A) Representative photographs of the electrophoresis of RT-PCR products of VEGF, IL-1α, and TNFα of control and 7ND-treated mice at Day 13. (B) The pooled data of the effects of 7ND treatment on mRNA expressions. Bar = 1 × SM ($n = 5$). $^{*}p < 0.05$ and $^{**}p < 0.01$ vs. control.

noma by inducing VEGF and inflammatory cytokines, including IL-1α and TNFα, through the TAM recruitment and the direct autocrine/paracrine effects on melanoma cells. The present study raises the possibility that inhibition of MCP-1 might be an adjunctive therapy for malignant melanoma.

Acknowledgments

Sources of support: this study was supported in part by a grant for the Science Frontier Research Promotion Centers (Cardiovascular Research Institute) and by Grant-in-Aid for Scientific Research (Drs. Kai and Egami) from the Ministry of Education, Science, Sports and Culture, Japan.

References

[1] H. Torisu, M. Ono, H. Kiryu, M. Furue, Y. Ohmoto, J. Nakayama, Y. Nishioka, S. Sone, M. Kuwano, Macrophage infiltration correlates with tumor stage and angiogenesis in human malignant melanoma: possible involvement of TNFα and IL-1α, Int. J. Cancer 85 (2000) 182–188.

[2] R. Denjin, D.J. Reiter, The possible role of angiogenesis in the metastatic potential of human melanoma. Clinicopathological aspects, Melanoma Res. 3 (1993) 5–14.

[3] J. Folkman, Angiogenesis in cancer, vascular, rheumatoid and other disease, Nat. Med. 1 (1995) 27–31.

[4] D.F.J. Hanahan, Patterns and emerging mechanisms of the angiogenic switch during tumorigenesis, Cell 86 (1996) 353–364.

[5] N. Ferrara, R.S. Kerbel, Angiogenesis as a therapeutic target, Nature 438 (2005) 967–973.

[6] R.D. Leek, C.E. Lewis, R. Whitehouse, M. Greenall, J. Clarke, A.L. Harris, Association of macrophage infiltration with angiogenesis and prognosis in invasive breast carcinoma, Cancer Res. 56 (1996) 4625–4629.

[7] R.P. Negus, G.W. Stamp, J. Hadley, F.R. Balkwill, Quantitative assessment of the leukocyte infiltrate in ovarian cancer and its relationship to the expression of C–C chemokines, Am. J. Pathol. 150 (1997) 1723–1734.

[8] L. Mazzucchelli, P. Loetscher, A. Kappeler, M. Uguccioni, M. Baggiolini, J.A. Laissue, C. Mueller, Monocyte chemoattractant

protein-1 gene expression in prostatic hyperplasia and prostate adenocarcinoma, Am. J. Pathol. 149 (1996) 501–509.
[9] V. Goede, L. Brogelli, M. Ziche, H.G. Augustin, Induction of inflammatory angiogenesis by monocyte chemoattractant protein-1, Int. J. Cancer 82 (1999) 765–770.
[10] H. Saji, M. Koike, T. Yamori, S. Saji, M. Seiki, K. Matsushima, M. Toi, Significant correlation of monocyte chemoattractant protein-1 expression with neovascularization and progression of breast carcinoma, Cancer 92 (2001) 1085–1091.
[11] L. Bingle, C.E. Lewis, K.P. Corke, M.W. Reed, N.J. Brown, Macrophages promote angiogenesis in human breast tumour spheroids in vivo, Br. J. Cancer 94 (2006) 101–107.
[12] E. Nakashima, K. Mukaide, Y. Kubota, K. Kuno, K. Yasumoto, F. Ichimura, I. Nakanishi, M. Miyasaka, K. Matsushima, Human MACF gene transfer enhances the metastatic capacity of a mouse cachectic adenocarcinoma cell line in vivo, Pharm. Res. 12 (1995) 1598–1604.
[13] T. Valkovic, K. Lucin, M. Krstulja, R. Dobi-Babic, N. Jonjic, Expression of monocyte chemotactic protein-1 in human invasive ductal breast cancer, Pathol. Res. Pract. 194 (1998) 335–340.
[14] Y. Zhang, B.J. Rollins, A dominant negative inhibitor indicates that monocyte chemoattractant protein 1 function as a dimer, Mol. Cell. Biol. 15 (1995) 4851–4855.
[15] K. Egashira, M. Koyanagi, S. Kitamoto, W. Ni, C. Kataoka, R. Morishita, Y. Kaneda, C. Akiyama, K. Nishida, K. Sueishi, A. Takeshita, Anti-monocyte chemoattractant protein-1 gene therapy inhibits vascular remodeling in rats: blockade of MCP-1 activity after intramuscular transfer of a mutant gene inhibits vascular remodeling induced by chronic blockade of NO synthesis, FASEB J. 14 (2000) 1974–1978.
[16] W. Ni, K. Egashira, S. Kitamoto, C. Kataoka, M. Koyanagi, S. Inoue, K. Imaizumi, C. Akiyama, K. Nishida, A. Takeshita, New anti-monocyte chemoattractant protein-1 gene therapy attenuates atherosclerosis in apolipoprotein E-knockout mice, Circulation 103 (2001) 2096–2101.
[17] H. Niiyama, H. Kai, T. Yamamoto, T. Shimada, K. Sasaki, T. Murohara, K. Egashira, T. Imaizumi, Roles of endogenous monocyte chemoattractant protein-1 in ischemia-induced neovascularization, J. Am. Coll. Cardiol. 44 (2004) 661–666.
[18] C.S. Williams, M. Tsujii, J. Reese, S.K. Dey, R.N. DuBois, Host cyclooxygenase-2 modulates carcinoma growth, J. Clin. Invest. 105 (2000) 1589–1594.
[19] K. Egami, T. Murohara, T. Shimada, K. Sasaki, S. Shintani, T. Sugaya, M. Ishii, T. Akagi, H. Ikeda, T. Matsuishi, T. Imaizumi, Role of host angiotensin II type 1 receptor in tumor angiogenesis and growth, J. Clin. Invest. 112 (2003) 67–75.
[20] N. Tahara, H. Kai, H. Niiyama, T. Mori, Y. Sugi, N. Takayama, H. Yasukawa, Y. Numaguchi, H. Matsui, K. Okamura, T. Imaizumi, Repeated gene transfers of naked prostacyclin synthase plasmid into skeletal muscles attenuate monocrotaline-induced pulmonary hypertension and prolong survival in rats, Hum. Gene Ther. 15 (2004) 1270–1278.
[21] I. Danko, J.D. Fritz, S. Jiao, K. Hogan, J.S. Latendresse, J.A. Wolff, Pharmacological enhancement of in vivo foreign gene expression in muscle, Gene Ther. 1 (1994) 114–121.
[22] J. Wang, L. Sun, L. Myeroff, X. Wang, L.E. Gentry, J. Yang, J. Liang, E. Zborowska, S. Markowitz, J.K. Willson, M.G. Brattain, Demonstration that mutation of the type II transforming growth factor beta receptor inactivates its tumor suppressor activity in replication error-positive colon carcinoma cells, J. Biol. Chem. 270 (1995) 22044–22049.
[23] M. Koga, H. Kai, H. Yasukawa, T. Yamamoto, Y. Kawai, S. Kato, K. Kusaba, M. Kai, K. Egashira, T. Kataoka, T. Imaizumi, Inhibition of progression and stabilization of plaques by postnatal interferon-γ function blocking in ApoE-knockout mice, Circ. Res. 101 (2007) 348–356.
[24] K. Kusaba, H. Kai, M. Koga, N. Takayama, A. Ikeda, H. Yasukawa, Y. Seki, K. Egashira, T. Imaizumi, Inhibition of intrinsic interferon-γ function prevents neointima formation after balloon injury, Hypertension 49 (2007) 909–915.
[25] F. Kuwahara, H. Kai, K. Tokuda, M. Kai, A. Takeshita, K. Egashira, T. Imaizumi, Transforming growth factor-β function blocking prevents myocardial fibrosis and diastolic dysfunction in pressure-overloaded rats, Circulation 106 (2002) 130–135.
[26] S. Nakao, T. Kuwano, C. Tsutsumi-Miyahara, S. Ueda, Y.N. Kimura, S. Hamano, K.H. Sonoda, Y. Saijo, T. Nukiwa, R.M. Strieter, T. Ishibashi, M. Kuwano, M. Ono, Infiltration of COX-2-expressing macrophages is a prerequisite for IL-1 beta-induced neovascularization and tumor growth, J. Clin. Invest. 115 (2007) 2979–2991.
[27] V.C. Grav-Schopfer, M. Karasarides, R. Havward, R. Marais, Tumor necrosis factor-alpha blocks apoptosis in melanoma cells when BRAF signal is inhibited, Cancer Res. 67 (2007) 122–129.
[28] D.M. Elaraj, D.M. Weinreich, S. Varghese, M. Puhlmann, S.M. Hewitt, N.M. Carroll, E.D. Feldman, E.M. Turner, H.R. Alexander, The role of interleukin 1 in growth and metastasis of human cancer xenografts, Clin. Cancer Res. 12 (2006) 1088–1096.
[29] Y.N. Kimura, K. Watari, A. Fotovati, F. Hosoi, K. Yasumoto, H. Izumi, K. Kohno, K. Umezawa, H. Iguchi, K. Shirouzu, S. Takamori, M. Kuwano, M. Ono, Inflammatory stimuli from macrophages and cancer cells synergistically promote tumor growth and angiogenesis, Cancer Sci. (2007) 9 (Epub ahead of print 2007).
[30] R. Salcedo, M.L. Ponce, H.A. Young, K. Wasserman, J.M. Ward, H.K. Kleinman, Human endothelial cells express CCR2 and respond to MCP-1: direct role of MCP-1 in angiogenesis and tumor progression, Blood 96 (2000) 34–40.

Pharmaceutical Research, Vol. 24, No. 6, June 2007 (© 2007)
DOI: 10.1007/s11095-007-9235-2

Research Paper

The Identification of Two Germ-line Mutations in the *Human Breast Cancer Resistance Protein* Gene that Result in the Expression of a Low/Non-functional Protein

Sho Yoshioka,[1] Kazuhiro Katayama,[1] Chikako Okawa,[1] Sachiko Takahashi,[1] Satomi Tsukahara,[2] Junko Mitsuhashi,[1,2] and Yoshikazu Sugimoto[1,2,3]

Received September 11, 2006; accepted January 2, 2007; published online March 21, 2007

Purpose. We examined the effects of the nine nonsynonymous germ-line mutations/SNPs in the *breast cancer resistance protein (BCRP/ABCG2)* gene on the expression and function of the protein.
Materials and Methods. We generated cDNAs for each of these mutants (G151T, C458T, C496G, A616C, T623C, T742C, T1291C, A1768T, and G1858A *BCRP*) and compared the effects of their exogenous expression in PA317 cells with a wild-type control.
Results. PA/F208S cells (T623C *BCRP*-transfectants) expressed marginal levels of a BCRP protein species (65 kDa), which is slightly smaller than wild-type (70 kDa), but this mutant did not appear on the cell surface or confer drug resistance. PA/F431L cells (T1291C *BCRP*-transfectants) were found to express both 70 kDa and 65 kDa BCRP protein products. In addition, although PA/F431L cells expressed 70 kDa BCRP at comparable levels to PA/WT cells, they showed only marginal resistance to SN-38. PA/T153M cells (C458T *BCRP*-transfectants) and PA/D620N cells (G1858A *BCRP*-transfectants) expressed lower amounts of BCRP and showed lower levels of resistance to SN-38 compared with PA/WT cells.
Conclusions. We have shown that T623C *BCRP* encodes a non-functional BCRP and that T1291C *BCRP* encodes a low-functional BCRP. Hence, these mutations may affect the pharmacokinetics of BCRP substrates in patients harboring these alleles.

KEY WORDS: BCRP/ABCG2; drug resistance; SN-38; SNPs.

INTRODUCTION

ATP binding cassette (ABC) transporters, such as P-glycoprotein (P-gp) and MRP1, are responsible for the acquisition of multidrug resistance in cancer cells (1–3). These transporters pump out various structurally unrelated anticancer drugs in an ATP-dependent manner. Breast cancer resistance protein (BCRP/ABCG2) is a half-molecule ABC transporter harboring an N-terminal ATP binding domain and a C-terminal transmembrane domain that mediates resistance to SN-38 (an active metabolite of irinotecan), mitoxantron, and topotecan (4–8). We previously reported that BCRP forms a homodimer via Cys-603 interactions and that these homodimeric complexes function as an efflux pump for anticancer agents (9,10). We have also reported earlier that BCRP exports sulfated estrogens, suggesting that there is a physiological role of BCRP for the tissue distribution and excretion of steroid hormones (11). BCRP is also widely expressed in normal human tissues such as the placenta, intestine, kidney, liver, prostate, ovary, testis, and hematopoietic stem cells (5,12,13). BCRP is assumed to play a role in the protective functions of the maternal-placental barrier, blood-testis barrier and hematopoietic stem cells against toxic substances and metabolites (14,15). BCRP has also shown to be expressed in the mammary gland during lactation and, it seems to be responsible for the active secretion of the BCRP substrates into milk (16).

In our previous study, we identified three nonsynonymous SNPs within the *BCRP* gene, G34A substituting Met for Val-12 (V12M), C376T substituting a stop codon for Gln-126 (Q126Stop), and C421A substituting Lys for Gln-141 (Q141K). G34A *BCRP* cDNA-transfected cells were found to express similar amounts of BCRP protein and further showed similar levels of SN-38 resistance compared with wild-type *BCRP* cDNA-transfected cells. In contrast C376T *BCRP* cDNA encodes a nonfunctional protein and C421A *BCRP* cDNA-transfected cells expressed a lower amount of BCRP protein and showed lower resistance to SN-38 than wild-type *BCRP* transfected cells (17). More-

[1] Department of Chemotherapy, Kyoritsu University of Pharmacy, 1-5-30 Shibakoen, Minato-ku, Tokyo, 105-8512, Japan.
[2] Division of Gene Therapy, Cancer Chemotherapy Center, Japanese Foundation for Cancer Research, Tokyo, Japan.
[3] To whom correspondence should be addressed. (e-mail: sugimoto-ys@kyoritsu-ph.ac.jp)

ABBREVIATIONS: ABC transporter, ATP-binding cassette transmembrane transporter; BCRP, breast cancer resistance protein; DHFR, dihydrofolate reductase; GAPDH, glyceraldehyde-3-phosphate dehydrogenase; IRES, internal ribosome entry site; SNPs, single nucleotide polymorphisms.

Table I. Frequencies of Germ-line Mutations/SNPs Within The *BCRP* Gene

Variation		Frequency (%)	Number	Population	Reference
Nucleotide	Amino acid				
G34A	V12M	19	29	Japanese	17
G151T	G51C	0.1[a]	350	Japanese	
C376T	Q126Stop	1.2	124	Japanese	17
C421A	Q141K	26.6	124	Japanese	17
C458T	T153M	3.3	30	Cell line	32
C496G	Q166E	0.3[a]	200	Japanese	
A616C	I206L	20	10	Hispanic	33
T623C	F208S	0.3[a]	200	Japanese	
T742C	S248P	0.5[a]	200	Japanese	
T1291C	F431L	0.6[b]	260	Japanese	34
A1768T	N590Y	1.1	88	Caucasians	33
G1858A	D620N	1.1	90	unknown	35

[a] Determined in this study.
[b] Determined in this study and in previous reports (frequencies and patient numbers are combined).

over, as C421A *BCRP* expresses low levels of protein, it was reported to affect the pharmacokinetics of patients harboring this allele who had been treated with an intracavernous administration of difromotecan (18). C421A *BCRP* was also reported to affect the pharmacokinetics of rosuvastain in healthy Chinese males (19).

In our present study, we generated nine *BCRP* cDNAs, each carrying a nonsynonymous germ-line mutation/SNP that has been already published or reported in a database. The effects of these different mutations on BCRP expression and function were examined in cells exogenously expressing these cDNAs.

MATERIALS AND METHODS

BCRP Expression Vectors

We generated nine cDNAs corresponding to the *BCRP* germ-line mutations/SNPs, G151T, C458T, C496G, A616C, T623C, T742C, T1291C, A1768T, G1858A [Table I (17), (32–35)]. G34A and C421A *BCRP* cDNAs were also used as controls. These *BCRP* germ-line mutations/SNPs have been described previously, some are in publication and the others are in the database of National Center for Biotechnology Information. For the transfection of these *BCRP* cDNA species, we generated bicistronic constructs using the pHa-IRES-DHFR vector. Mutant *BCRP* cDNAs were then prepared using the Mutan-Super Express Km site-directed mutagenesis system (Takara, Ohtsu, Japan) as directed by the manufacturer's instructions. Either wild-type or germ-line mutation/SNP-containing *BCRP* cDNAs without any other mutations were subsequently inserted into the pHa-IRES-DHFR bicistronic retrovirus vector that carries *DHFR* cDNA.

Cell Culture Conditions and Establishment of *BCRP* Transfectants

Murine fibroblast PA317 cells were cultured in Dulbecco's modified eagle medium supplemented with 7% fetal bovine serum at 37°C in a humidified 5% CO_2 environment. For the establishment of both wild-type and mutant *BCRP* transfectants, PA317 cells were transfected with pHa-BCRP-IRES-DHFR constructs containing either wild-type, G34A, G151T, C421A, C458T, A616C, T623C, T742C, T1291C, A1768T, or G1858A *BCRP* cDNA using a MBS Mammalian Transfection Kit (Stratagene, La Jolla, CA). The cells were selected with 120 ng/mL of methotrexate, and the resulting mixed populations of resistant cells were designated as PA/WT, PA/V12M, PA/G51C, PA/Q141K, PA/T153M, PA/I206L, PA/F208S, PA/S248P, PA/F431L, PA/N590Y and PA/D620N, respectively. The PA/F208S clones and PA/F431L clones were obtained by limiting dilution.

Cell Growth Inhibition Assay

Anticancer agent resistance levels in both the parental PA317 cells and in the various BCRP transfectants were

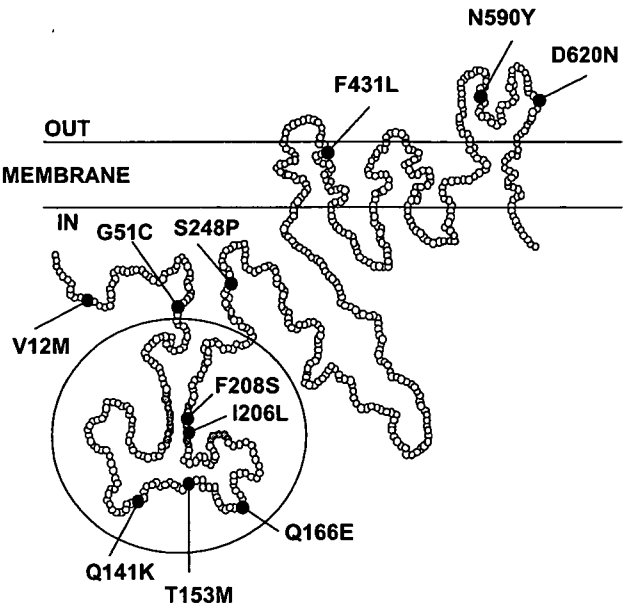

Fig. 1. Schematic representation of the breast cancer resistance protein and locations of the germ-line mutations/SNPs analyzed in this study.

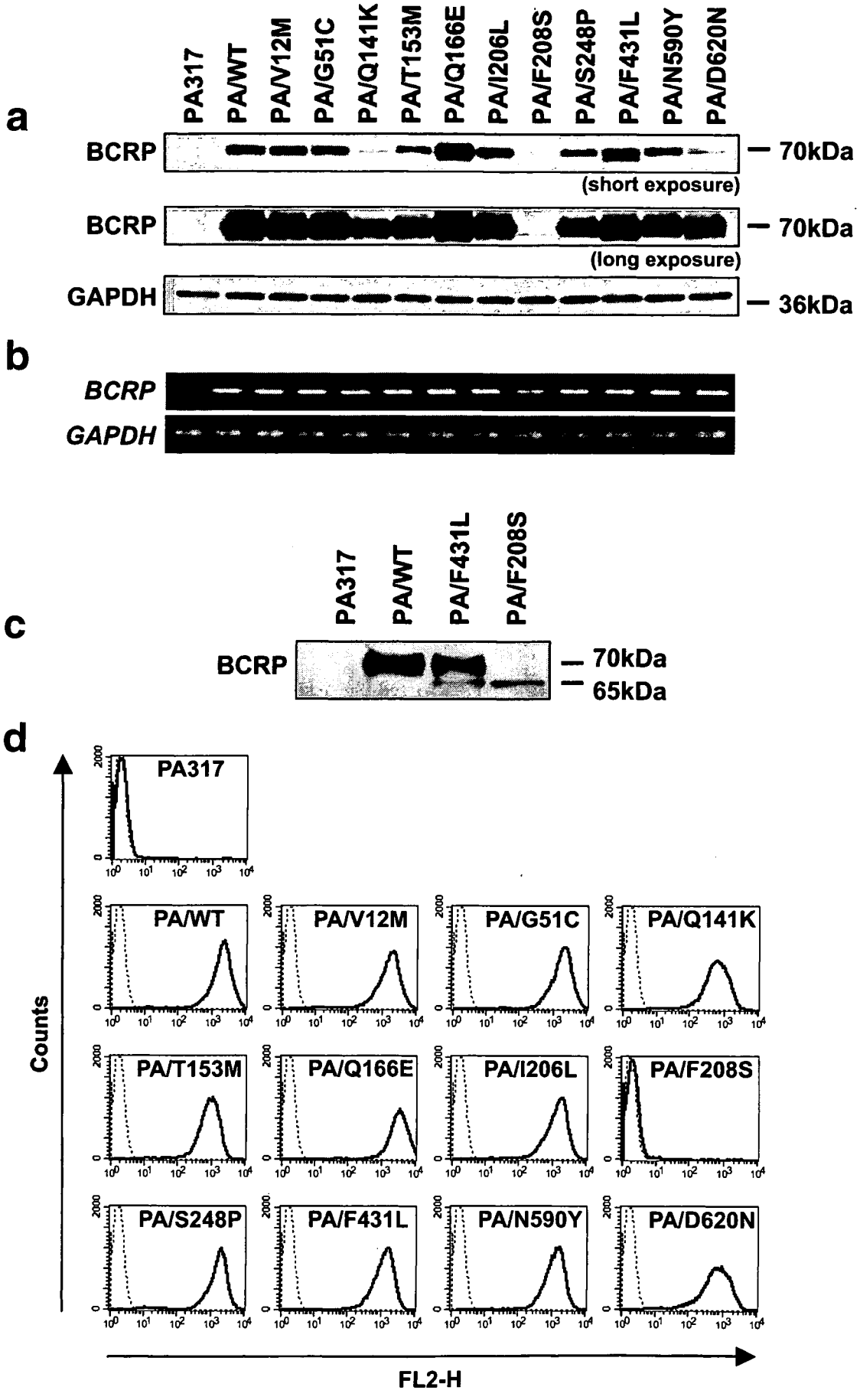
a
PA317
PA/WT
PA/V12M
PA/G51C
PA/Q141K
PA/T153M
PA/Q166E
PA/I206L
PA/F208S
PA/S248P
PA/F431L
PA/N590Y
PA/D620N
BCRP
70kDa
(short exposure)
BCRP
70kDa
(long exposure)
GAPDH
36kDa
b
BCRP
GAPDH
c
PA317
PA/WT
PA/F431L
PA/F208S
BCRP
70kDa
65kDa
d
Counts
PA317
PA/WT
PA/V12M
PA/G51C
PA/Q141K
PA/T153M
PA/Q166E
PA/I206L
PA/F208S
PA/S248P
PA/F431L
PA/N590Y
PA/D620N
FL2-H

evaluated by cell growth inhibition assays after incubation of the cells for 5 days at 37°C in the absence or presence of various concentrations of SN-38 (Yakult Honsha, Tokyo). Cell numbers were determined with a Coulter counter (Sysmex, Kobe, Japan). IC_{50} values (drug dose causing 50% inhibition of cell growth) were determined from growth inhibition curves.

Western Blotting

Cell lysates were obtained as described previously (10). Cell lysates from the *BCRP* transfectants were resolved by SDS-PAGE and then electro-transferred onto a nitrocellulose membrane. The membrane was incubated with 1 μg/mL of anti-BCRP polyclonal antibody 3488 (9) and a GAPDH mouse monoclonal antibody as an internal control, followed by washing and treatment with peroxidase-conjugated sheep anti-rabbit and anti-mouse secondary antibody (Amersham, Buckinghamshire, UK), respectively. The membrane-bound antibodies were visualized with the Enhanced Chemiluminescence (ECL) Plus Western blotting detection system (Amersham).

Fluorescence-activated Cell Sorting (FACS) Analysis of BCRP Expression

The expression levels of human BCRP on the cell surfaces of various *BCRP* transfectants were examined by FACS analysis using a human-specific anti-BCRP monoclonal antibody (eBiosciences, San, Diego, CA), that was raised against a cell surface epitope of BCRP. The cells were incubated with or without a biotinylated anti human ABCG2 (20 μg/mL) for 30 min on ice, followed by washing and incubation with R-phycoerythrin-conjugated streptavidin (400 μg/mL; BD Biosciences, Franklin Lakes, NJ) (20) for 30 min on ice. Fluorescence staining levels were measured using FACS Calibur (BD Biosciences).

Semi-quantitative Reverse Transcriptase Chain Reaction (RT-PCR) Analysis

The isolation of total RNA and subsequent RT-PCR analysis was performed using an RNeasy kit (Qiagen, Valencia, CA) and an RNA LA PCR kit (Takara), respectively, according to the manufacturer's instructions. First-strand *BCRP* cDNA was synthesized from 0.3 μg of total RNA and a 824 bp *BCRP* cDNA fragment was amplified by PCR with the forward and reverse primers, 5′-GATATCAATGATACAGGGTT-3′ and 5′-TGTCCAATAGAATATTCCCC-3′, respectively. The PCR conditions were as follows: 95°C for 5 min, followed by 18–24 cycles of 95°C for 30 sec, 55°C for 30 sec and 72°C for 1 min, and a final extension for 7 min at 72°C. As an internal control, the amplification of *GAPDH* cDNA (551 bp fragment) was carried out using the same procedure.

Table II. SN-38 Resistance Levels of PA317 Transfectants[a]

Cell type	IC_{50} (nmol/L)	Degree of resistance
PA317	11±0.2	1
PA/WT	550±16	50
PA/V12M	490±13	45
PA/Q141K	110±5.9	10
PA/T153M	260±15	24
PA/Q166E	680±40	62
PA/F208S	10±0.7	1
PA/F431L	34±0.9	3
PA/D620N	190±5.7	17

[a] Cells were cultured for 5 days with various concentrations of SN-38. Cell numbers were then measured using a Coulter counter, and the IC_{50} values were determined. The degree of drug resistance is calculated as the IC_{50} ratio of resistant cells divided by that of the parental cells. The data are represented as the mean ± SD from triplicate determinations.

Sequencing Analysis of the *BCRP* Gene

Peripheral blood nucleated cells were obtained from both healthy volunteers and cancer patients of Japanese nationality, after obtaining written informed consent, to undertake genetic analysis from each of these individuals. Exon 2 of the *BCRP* gene, which covers the 151st nucleotide of *BCRP* cDNA, was amplified by PCR with the primer set, forward; 5′-GCAATCTCATTTATCTGGACTA-3′ and reverse; 5′-TGTGAGGTTCACTGTAGGTAAA-3′. Exon 5 of the *BCRP* gene, which covers the 496th nucleotide of *BCRP* cDNA was amplified by PCR with the primer set, forward; 5′-CCTTAGTTATGTTATCTTTGTG-3′ and reverse; 5′-GAAACTTCTGAATCAGAGTCAT-3′. Exon 6 of the *BCRP* gene, which covers the 623rd nucleotide of *BCRP* cDNA was amplified by PCR with the primer set, forward; 5′-GCTCACCAAATGATAATGACT-3′ and reverse; 5′-TGGGACATAGTAGTGATAAGA-3; Exon 7 of the *BCRP* gene, which covers the 742nd nucleotide of *BCRP* cDNA was amplified by PCR with the primer set, forward; 5′-GAGCAAACAATCTAAAGGCAA-3′ and reverse; 5′-ACCCAAAGACCAAACAGCACT-3′. Exon 11 of the *BCRP* gene, which covers the 1291st nucleotide of *BCRP* cDNA was amplified by PCR with the primer set, forward; 5′-CTGTCTAAGAATGCTGAGTTG-3′ and revere; 5′-ATCAGTCTAACCAATAGCCCC-3′. The resulting PCR products were directly sequenced using the following primers, which were designed from the respective intronic sequences; 5′-AACTTACTATTGCTTTTCTGTC-3′ (from

◀ **Fig. 2.** BCRP protein and mRNA expression in PA317 transfectants. **a**, Western blot analysis of BCRP in each of the *BCRP* transfectants. Protein samples (20 μg) were subjected to western blotting using the rabbit anti-BCRP polyclonal antibody (3488) or a mouse anti-GAPDH monoclonal antibody. The short and long exposures indicated were of 5 min and 15 min duration on X-ray film, respectively. **b**, Semi-quantitative RT-PCR of *BCRP* mRNA in the PA317 transfectants. The *BCRP* (824 bp) and *GAPDH* (551 bp) transcripts were amplified by RT-PCR from 0.3 μg of total RNA. **c**, Western blot analysis of BCRP in PA317, PA/WT, PA/F431L, and PA/F208S cells as described above. **d**, BCRP cell surface expression analysis in the PA317 transfectants by FACS. Parental PA317 cells and corresponding *BCRP* transfectants were harvested and then incubated with (*bold line*) or without (*dotted line*) a biotinylated anti-human BCRP monoclonal antibody 5D3, followed by treatment with R-phycoerythrin-conjugated streptavidin. After washing, the fluorescence intensities were measured using FACS Calibur.

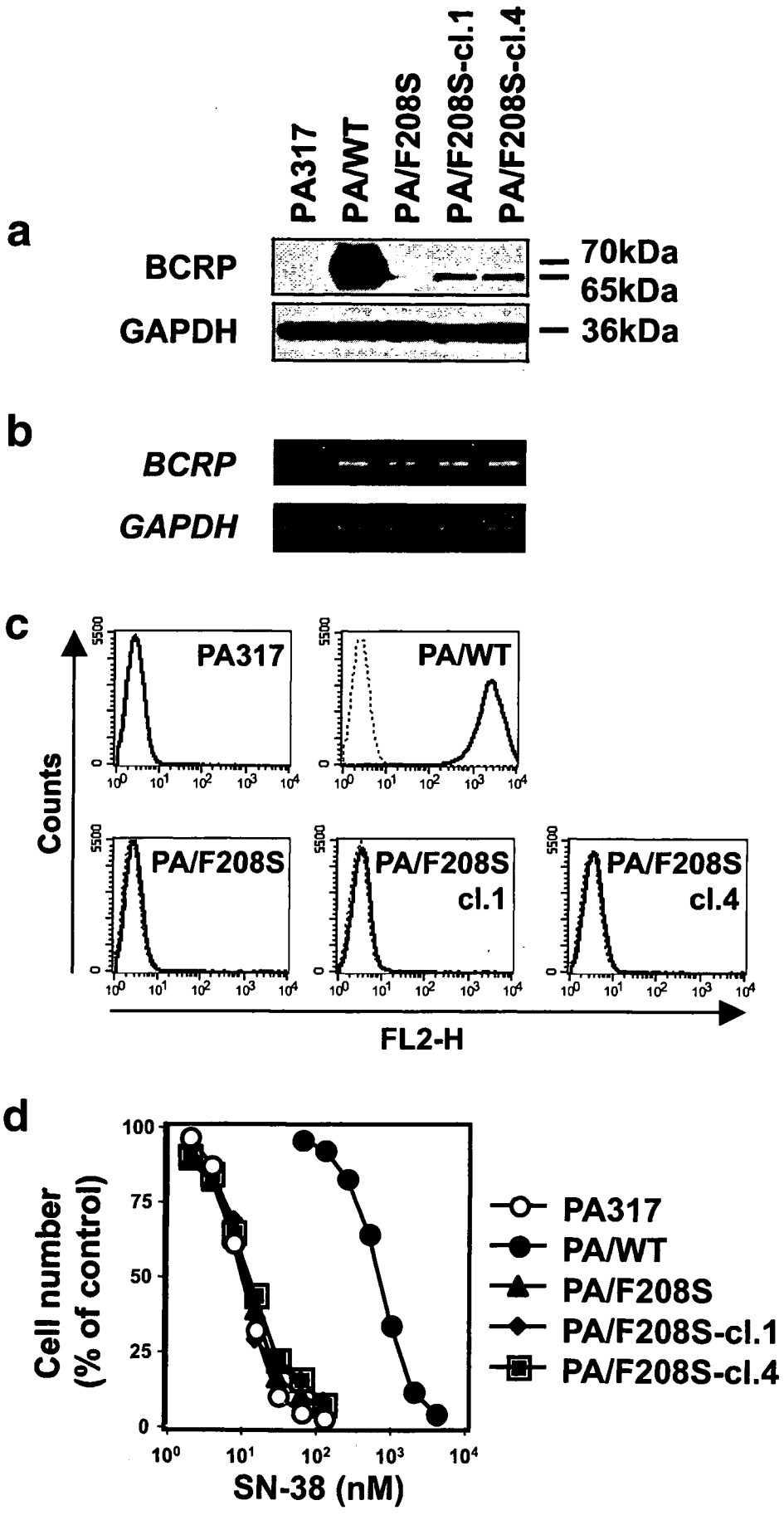
a
PA317
PA/WT
PA/F208S
PA/F208S-cl.1
PA/F208S-cl.4
BCRP
GAPDH
70kDa
65kDa
36kDa
b
BCRP
GAPDH
c
PA317
PA/WT
PA/F208S
PA/F208S cl.1
PA/F208S cl.4
Counts
FL2-H
d
Cell number (% of control)
SN-38 (nM)
PA317
PA/WT
PA/F208S
PA/F208S-cl.1
PA/F208S-cl.4

−46 to −25 upstream of exon 2), 5′-CTAAACAGT-CATGGTCTTAGAAA-3′(from −68 to −46 upstream of exon 5), 5′-AAATGATAATGACTGGTTGTT-3′(from −52 to −32 upstream of exon 6), 5′-AAGAATAGAGTATTT-TACTGAGA-3′(from −75 to −53 upstream of exon 7), 5′-CTAAGAATGCTGAGTTGACTG-3′(from −50 to −30 upstream of exon 11).

RESULTS

Expression of BCRP in PA317 Transfectants

The germ-line mutations and resulting amino acid substitutions examined in this study were as follows; G151T (G51C), C458T (T153M), C496G (Q166E), A616C (I206L), T623C (F208S), T742C (S248P), T1291C (F431L), A1768T (N590Y) and G1858A (D620N). G51C, T153M, Q166E, I206L, F208S and S248P are located in the intracellular domain of the protein (Fig. 1 and Table I). F431L, N590Y and D620N are located within the transmembrane domain (Fig. 1 and Table I).

BCRP expression levels in each of the PA317 transfectants were then examined by western blotting. The wild-type *BCRP* transfectants (PA/WT) express a 70-kDa BCRP species (Fig. 2a). Similar to previous findings (14), PA/V12M cells were observed to express similar amounts of BCRP compared with PA/WT cells, whereas PA/Q141K cells expressed significantly lower amounts of BCRP than PA/WT (Fig. 2a). Among the 11 mutant BCRP transfectants under study, PA/F208S cells were found to express the lowest levels of BCRP, corresponding to a 65-kDa protein (Fig. 2a and c). PA/F431L expressed BCRP products of two distinct molecular sizes, 70-kDa and 65-kDa (Fig. 2a and c). PA/T153M and PA/D620N transfectants expressed lower amounts of BCRP than PA/WT cells, but these levels were higher than those in the PA/Q141K cells (Fig. 2a). PA/Q166E cells expressed higher amounts of BCRP (70-kDa) than PA/WT cells (Fig. 2a). The remaining transfectants PA/G51C, PA/I206L, PA/S248P, and PA/N590Y expressed BCRP at levels that were comparable to PA/WT cells (Fig. 2a).

The BCRP mRNA expression levels in each of the transfectants were analyzed by RT-PCR. As shown in Fig. 2b, the 11 mutant *BCRP* transfectants expressed *BCRP* transcript levels that were comparable to PA/WT cells (Fig. 2b).

◀ **Fig. 3.** BCRP protein and mRNA expression in PA/F208S clones. **a**, Western blot analysis of BCRP in PA/208S clones. Protein samples (20 μg) were subjected to western blotting using either a rabbit anti-BCRP polyclonal antibody 3488 or a mouse anti-GAPDH monoclonal antibody. **b**, Semi-quantitative RT-PCR analysis of *BCRP* mRNA in the indicated PA/F208S clones. The *BCRP* (824 bp) and *GAPDH* (551 bp) transcripts were amplified by RT-PCR from 0.3 μg of total RNA. **c**, BCRP cell surface expression analysis of PA/F208S clones by FACS as described for Fig. 2d. **d**, Drug resistance levels for the PA/F208S clones. PA317 (*open circle*), PA/WT (*closed circle*), PA/F208S (*closed triangle*), PA/F208S clone 1 (*closed lozenge*), and clone 4 (*closed square*) cells were cultured for 5 days with various concentrations of SN-38. Cell numbers were determined using a Coulter counter. Data are represented by the mean ± SD from triplicate experiments.

Cell Surface BCRP Expression in the Mutant *BCRP* Transfectants

The expression levels of BCRP on the cell surfaces of each of the transfectants were examined by FACS and were undetectable in either the PA/F208S or parental PA317 cells (Fig. 2d). PA/Q141K, PA/T153M and PA/D620N cells expressed lower amounts of BCRP on their cell surfaces than PA/WT cells (Fig. 2d). These results were consistent with the immunoblotting analysis (Fig. 2a). The cell surface expression of BCRP in PA/Q166E cells was slightly higher compared with PA/WT cells (Fig. 2d). Each of the other transfectants (PA/G51C, PA/I206L, PA/S248P, PA/F431L, and PA/N590Y cells) showed similar cell surface BCRP expression levels to PA/WT (Fig. 2d).

Drug Resistance of Mutant *BCRP* Transfectants

The resistance of each of the *BCPR* transfectants to SN-38 was analyzed by cell growth inhibition assay. PA/WT cells showed a 50-fold higher resistance to SN-38 than the parental PA317 cells (Table II). PA/F208S cells showed a similar level of SN-38 sensitivity to PA317 cells (Table II). PA/F431L cells showed 3-fold higher resistance to SN-38 than PA317 cells but PA/F431L cells were found to be 15-fold more sensitive to this agent than PA/WT cells (Table II). PA/Q141K, PA/T153M, and PA/D620N cells showed 10–24-fold higher resistance levels to SN-38 compared with the parental cells (Table II). However, these cells were 2–5 times more sensitive to SN-38 when compared with PA/WT cells (Table II). Additional transfectants (PA/G51C, PA/Q166E, PA/I206L, PA/S248P, and PA/N590Y cells) showed no change in their drug resistance profiles to SN-38 compared with PA/WT cells (Table II).

Analyses of PA/F208S Subclones

We isolated two independent clones from the population of PA/F208S cells, (PA/F208S-cl.1 and -cl.4) that expressed higher levels of 65-kDa BCRP protein than PA/F208S cells by western blot (Fig. 3a), but the cell surface expression of BCRP were not detectable in these clones by FACS analysis (Fig. 3c). In addition, these clones did not show SN-38 resistance (Fig. 3d).

Analyses of PA/F431L Clones

PA/F431L cells expressed two species of BCRP of molecular weights 70- and 65-kDa (Fig. 2a). To confirm whether these two versions of the protein were derived from a single gene, we isolated independent PA/F431L subclones, PA/F431L-cl.6 and -cl.15. As shown in Fig. 4a, both of these clones simultaneously expressed the 70- and 65-kDa BCRP species, similar to the original mass population of PA/F431L cells. FACS analysis further revealed that these clones also showed similar BCRP expression levels on their cell surfaces to PA/WT and PA/F431L cells (Fig. 4c). Moreover, these clones showed no change in their exogenous *BCRP* mRNA levels compared with PA/WT and PA/F431L (Fig. 4b) but showed only marginal resistance to SN-38 treatment (Fig. 4d).

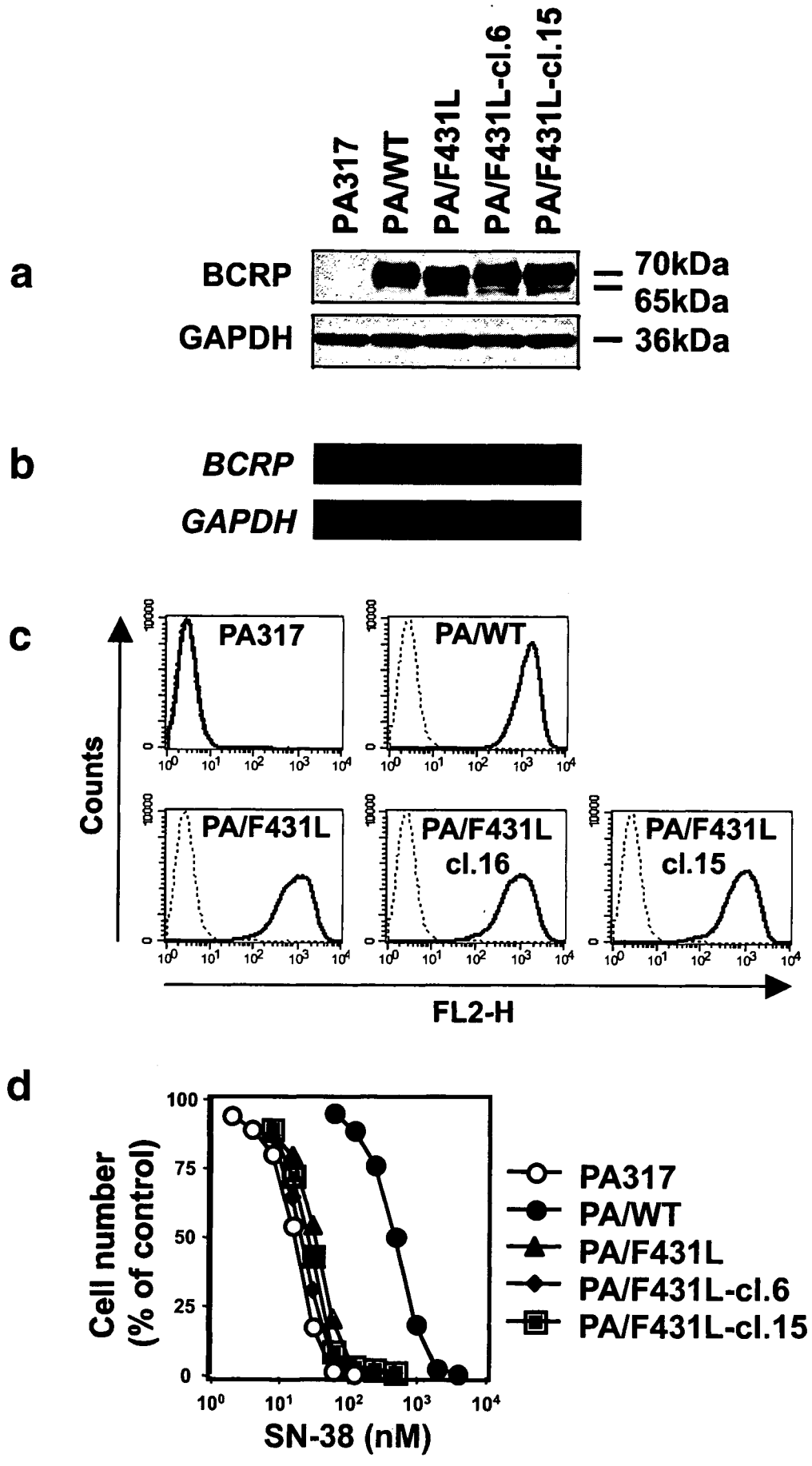
a
PA317
PA/WT
PA/F431L
PA/F431L-cl.6
PA/F431L-cl.15
BCRP
GAPDH
70kDa
65kDa
36kDa
b
BCRP
GAPDH
c
PA317
PA/WT
PA/F431L
PA/F431L cl.16
PA/F431L cl.15
Counts
FL2-H
d
Cell number (% of control)
SN-38 (nM)
PA317
PA/WT
PA/F431L
PA/F431L-cl.6
PA/F431L-cl.15

Frequencies of Germ-line Mutations Within the *BCRP* Gene

Due to the possible significance of the T623C and T1291C *BCRP* mutations, we examined the frequencies of five germ-line mutations, G151T, C496G, T623C, T742C and T1291C *BCRP*, among Japanese populations. We analyzed 200–350 samples in this study, depending on the frequency of each mutation. As shown in Table I, allele frequencies for the T623C *BCRP* and T1291C *BCRP* allele were 0.3% and 0.6%, respectively. A healthy volunteer was heterozygous for the T623C *BCRP* allele. Two healthy volunteer and a cancer patient were heterozygous for the T1291C *BCRP* allele. We previously reported that allele frequency for the C376T *BCRP*, that encodes a truncated protein, was 1.2% in the Japanese population (17). From both our previous and present results, we conclude that there are in fact two non-functional germ-line mutations/SNPs in the *BCRP* gene, C376T and T623C. It should be noted however that we have not thus far identified any individuals who are homozygous for either the C376T or T623C alleles, nor have we observed individuals who are heterozygous for a combination of these two alleles.

DISCUSSION

In our current study, we have examined the effect of the nine germ-line mutations/SNPs, G151T, C458T, C496G, A616C, T623C, T742C, T1291C, A1768T, and G1858A *BCRP*, resulting in the amino acid changes G51C, T153M, Q166E, I206L, F208S, S248P, F431L, N590Y, D620N, respectively, on BCRP protein expression and function. We first obtained both the wild-type and mutant *BCRP* cDNAs and expressed each in PA317 cells. The resulting mixed populations of cells were designated a PA/WT, PA/V12M, PA/G51C, PA/Q141K, PA/T153M, PA/I206L, PA/F208S, PA/S248P, PA/F431L, PA/N590Y and PA/D620N. PA/F208S cells were found to express marginal levels of BCRP (65-kDa) (Figs. 2a and 3a), which were slightly lower than wild-type BCRP, but did not appear on the cell surface (Figs. 2d and 3c). Moreover, PA/F208S cells did not show any drug resistance (Fig. 3c and Table II). PA/F431L cells expressed a 65-kDa and 70-kDa species of BCRP (Figs. 2a and 4a). In addition, although PA/F431L cells expressed BCRP at cell surface levels that were similar to PA/WT cells (Figs. 2d and 4c), they showed only marginal resistance to SN-38 (Fig. 4d and Table II). PA/T153M and PA/D620N cells expressed lower levels of BCRP and also showed lower resistance to SN-38, compared with PA/WT cells (Fig. 2a and Table II).

Our previously described bicistronic pHa-BCRP-IRES-DHFR construct (20–23) was used for the establishment of the mutant *BCRP* transfectants in the present study. In the resulting transfectants, *BCRP* and *DHFR* products are translated independently from single bicistronic mRNAs that are transcribed under the control of a retroviral long terminal repeat promoter. The upstream *BCRP* cDNA is translated in a cap-dependent manner, and the downstream *DHFR* is translated under the control of the IRES. Hence, cells expressing *DHFR*, resulting in methotrexate resistance, theoretically always coexpress the *BCRP* cDNA. It is noteworthy that methotrexate itself is reported to be a substrate of BCRP (24,25), but wild-type BCRP-transfected cells show only marginal resistance to this drug. In addition, BCRP expression does not affect the survival of cells transfected with the bicistronic DHFR vector, and mixed population of the methotrexate-resistant colonies (>100) were used in this study.

The amino acid positions of the germ-line mutations/SNPs examined in this study are represented by the black circles in Fig. 1. G51C, T153M, Q166E, I206L, F208S, and S248P are located in the intracellular domain, and F431L, N590Y, and D620N reside in the transmembrane domain. Walker A (80–89), Walker B (204–210), and Signature C (186–190) in the ATP binding site of BCRP are indicated by the gray circles in Fig. 1 and are conserved in other members of the ATP transporter family (26). The I206L BCRP and F208S BCRP mutants harbor amino acid substitutions within the Walker B region, which is likely to have a significant impact upon the functioning of the ATP binding site. PA/F208S cells express a marginal amount of a smaller BCRP protein species(65 kDa), which is not expressed on the cell surface (Figs. 2a, c, d, 3a and c). Moreover, PA/F208S cells do not show any drug resistant properties. Considering no expression of F208S BCRP mutant on the cell surface of PA/F208S, the lack of drug resistance property in the transfectant is probably due to the absence of cell surface transporter. On the other hand, PA/I206L cells show similar levels of BCRP expression and the resistance to SN-38 as PA/WT cells. Further studies are ongoing to evaluate the ATP-binding and -hydrolyzing activity of I206L BCRP and F208S BCRP mutants.

We recently examined the effects of a T3587G germ-line mutation in the human *MDR1* gene and found that the resulting I1196Y P-glycoprotein (P-gp), that also contains an amino acid substitution within the Walker B domain, did not have ATP-binding activity (27). In our T3587G *MDR1* transfectants, I1196S P-gp also did not appear on the cell surface, and the transfected cells were drug sensitive. These results are very similar to our current data for the T623C (F208S) *BCRP* germ-line mutation. Surprisingly, both the Ile residue of I1196Y P-gp and the Phe of F208S BCRP occupy the amino acid positions in the Walker B motifs of P-gp and BCRP, respectively. A number of ongoing studies in our laboratory are therefore currently focused on the mechanisms underlying the maturation and stability of mutant ABC transporters as this may have a significant impact upon the effectiveness of cancer chemotherapy regimens.

The loss of function of particular mutant ABC transporters has been extensively studied for multidrug resistance associated protein 2 (MRP2) in relation to Dubin-Johnson syndrome, an inherited disorder defined by chronic hyperbilirubinemia (28–30). R768W MRP2, which has the amino acid substitution in Signature C of the first ATP binding site of the protein, confers high serum bilirubin concentrations in the affected patients (28), and the mutant protein is not completely glycosylated (29). Q1382R MRP2 is a mutation

◀ **Fig. 4.** BCRP protein and mRNA expression in PA/F431L clones as described in Figs. 2 and 3. **a**, Western blot analysis of BCRP in PA/F431L clones **b**, Semi-quantitative RT-PCR of *BCRP* mRNA in PA/F431L clones. **c**, BCRP cell surface expression analysis of PA/F431L clones by FACS. **d**, Drug resistance levels in the PA/F431L clones. PA317 (*open circle*), PA/WT (*closed circle*), PA/F431L (*closed triangle*), PA/F431L clone 6 (*closed lozenge*), and PA/F431L clone 15 (*closed square*) cells were cultured for 5 days with various concentrations of SN-38 and assayed as described in Fig. 3d.

between the Walker A and the Signature C regions of the second ATP-binding site, and causes loss of ATP hydrolysis activity (29). Furthermore, the deletion of Arg-1392 and Met-1393 in MRP2, located between the Walker A and the Signature C regions of the second ATP-binding site, leads to both impaired maturation and trafficking of the protein (30). Based upon these earlier reports, it is evident that various amino acid substitutions in the ATP binding domain can result in a dysfunctional ABC transporter.

The F431L residue is located in the second transmembrane domain (Fig. 1) and PA/F431L cells express two species of BCRP of 70-kDa and 65-kDa in size. The 65-kDa F431L BCRP product has the same molecular weight as F208S BCRP by SDS-PAGE (Fig. 2a and c). From the results of our analysis of PA/F431L clones, these two products seemed to be generated from a single cDNA species (Fig. 4b). The 70-kDa BCRP expression levels in PA/F431L cells were also much higher than the 65-kDa BCRP protein in the same cells (Figs. 2c and 4c). Although PA/F431L cells express higher quantities of 70-kDa BCRP compared with PA/Q141K, PA/T153M, and PA/D620N cells (Fig. 2a) these cells in fact show a lower resistance to SN-38 than these other three transfectants (Table II). From these results, we speculate that this residue might in fact be important in the recognition of SN-38, and that the F431L substitution may result in lower transporter function than the wild-type protein. We previously reported that seven mutants of BCRP at residue E446, located in the second transmembrane domain, did not show any drug resistance and that 13 mutants of BCRP at R482, residing in the third transmembrane domain, showed higher resistance to mitoxantron and doxorubicin than wild-type BCRP (31).

PA/T153M and PA/D620N cells showed low-levels of BCRP expression and drug resistance to SN-38 compared with PA/WT cells (Fig. 2a and Table II). These results were similar to the data obtained for PA/Q141K cells and based upon these data, we hypothesize that the decrease in the resistance levels to SN-38 may not be due to functional alterations but to decreased protein expression. Similar results were obtained using NIH3T3/T153M and NIH3T3/D620N cells (date not shown).

The possible significance of the C421A *BCRP* was recently evaluated in a phase I study of diflomotecan, a new camptothecin derivative anticancer drug (18). In this study, five patients who were heterozygous for the C421A allele showed three-fold higher blood drug concentrations of diflomotecan than 15 patients who had wild-type allele (18). Following intravenous administration of this drug, the area-under-curve (AUC) of the individuals with the C421A allele and patients who were homozygous wild-type were 138 ng·h/mL and 46.1 ng·h/mL, respectively ($P = 0.015$). This study has therefore clearly shown that germ-line mutations/SNPs in the *BCRP* gene that cause a reduction in expression or loss of functions of the protein will alter the pharmacokinetics of BCRP substrate anticancer agents.

CONCLUSION

We have characterized two important *BCRP* germ-line mutations, T623C (F208S) and T1291C (F431L). T623C *BCRP* cDNA encodes a non-functional BCRP, and T1291C *BCRP* cDNA encodes a low-functional protein product. Polymorphisms within the *BCRP* genes of individuals that severely disrupt transporter activity are thus likely to be associated with hypersensitivity to substrate anticancer agents. Because BCRP may play crucial roles in the absorption and excretion of anticancer drugs, the monitoring of *BCRP* germ-line mutations/SNPs should be considered carefully during the clinical development of novel anticancer agents and BCRP-reversing drugs.

ACKNOWLEDGMENTS

This study was supported by the Ministry of Education, Culture, Sports, Science and Technology, and the Ministry of Health, Labor and Welfare, Japan.

REFERENCES

1. M. M. Gottesman, C. A. Hrycyna, P. V. Schoenlein, U. A. Germann, and I. Pastan. Genetic analysis of the multidrug transporter. *Annu. Rev. Genet.* **29**:607–649 (1995).
2. C. J. Chen, J. E. Chin, K. Ueda, D. P. Clark, I. Pastan, M. M. Gottesman, and I. B. Roninson. Internal duplication and homology with bacterial transport proteins in the mdr1 (P-glycoprotein) gene from multidrug-resistant human cells. *Cell* **47**:381–389 (1986).
3. S. P. Cole, G. Bhardwaj, J. H. Gerlach, J. E. Mackie, C. E. Grant, K. C. Almquist, A. J. Stewart, E. U. Kurz, A. M. Duncan, and R. G. Deeley. Overexpression of a transporter gene in a multidrug-resistant human lung cancer cell line. *Science* **258**:1650–1654 (1992).
4. R. Allikmets, L. M. Schriml, A. Hutchinson, V. Romano-Spica, and M. Dean. A human placenta-specific ATP-binding cassette gene (ABCP) on chromosome 4q22 that is involved in multidrug resistance. *Cancer Res.* **58**:5337–5339 (1998).
5. L. A. Doyle, W. Yang, L. V. Abruzzo, T. Krogmann, Y. Gao, A. K. Rishi, and D. D. Ross. A multidrug resistance transporter from human MCF-7 breast cancer cells. *Proc. Natl. Acad. Sci. U.S.A.* **95**:15665–15670 (1998).
6. K. Miyake, L. Mickley, T. Litman, Z. Zhan, R. Robey, B. Cristensen, M. Brangi, L. Greenberger, M. Dean, T. Fojo, and S. E. Beates. Molecular cloning of cDNAs which are highly overexpressed in mitoxantrone-resistant cells: demonstration of homology to ABC transport genes. *Cancer Res.* **59**:8–13 (1999).
7. M. Maliepaard, M. A. van Gastelen, L. A. de Jong, D. Pluim, R. C. van Waardenburg, M. C. Ruevekamp-Helmers, B. G. Floot, and J. H. Schellens. Overexpression of the BCRP/MXR/ABCP gene in a topotecan-selected ovarian tumor cell line. *Cancer Res.* **59**:4559–4563 (1999).
8. S. Kawabata, M. Oka, K. Shiozawa, K. Tsukamoto, K. Nakatomi, H. Soda, M. Fukuda, Y. Ikegami, K. Sugahara, Y. Yamada, S. Kamihira, L. A. Doyle, D. D. Ross, and S. Kohno. Breast cancer resistance protein directly confers SN-38 resistance of lung cancer cells. *Biochem. Biophys. Res. Commun.* **280**:1216–1223 (2001).
9. K. Kage, S. Tsukahara, T. Sugiyama, S. Asada, E. Ishikawa, T. Tsuruo, and Y. Sugimoto. Dominant-negative inhibition of breast cancer resistance protein as drug efflux pump through the inhibition of S-S dependent homodimerization. *Int. J. Cancer* **97**:626–630 (2002).
10. K. Kage, T. Fujita, and Y. Sugimoto. Role of Cys-603 in dimer/oligomer formation of the breast cancer resistance protein BCRP/ABCG2. *Cancer Sci.* **96**:866–872 (2005).
11. Y. Imai, S. Asada, S. Tsukahara, E. Ishikawa, T. Tsuruo, and Y. Sugimoto. Breast cancer resistance protein exports sulfated estrogens but not free estrogens. *Mol. Pharmacol.* **64**:610–618 (2003).
12. M. Maliepaard, G. L. Scheffer, I. F. Faneyte, M. A. Gastelenvan, A. C. Pijnenborg, A. H. Schinkel, M. J. Vijvervan De, R. J. Scheper, and J. H. Schellens. Subcellular localization and distribution of the breast cancer resistance protein transporter in normal human tissues. *Cancer Res.* **61**:3458–3464 (2001).
13. S. Zhou, J. D. Schuetz, K. D. Bunting, A. M. Colapietro, J. Sampath, J. J. Morris, I. Lagutinal, G. C. Grosveld, M. Osawa,

H. Nakauchi, and B. P. Sorrentino. The ABC transporter Bcrp1/ABCG2 is expressed in a wide variety of stem cells and is a molecular determinant of the side-population phenotype. *Nat. Med.* 7:1028–1034 (2001).
14. D. M. Kolkvan der, E. Vellenga, G. L. Scheffer, M. Muller, S. E. Bates, R. J. Scheper, and E. G. Vriesde. Expression and activity of breast cancer resistance protein (BCRP) in de novo and relapsed acute myeloid leukemia. *Blood* **99**:3763–3770 (2002).
15. M. M. van den Heuvel-Eibrink, E. A. Wiemer, A. Prins, J. P. Meijerink, P. J. Vossebeld, B. van der Holt, R. Pieters, P. Sonneveld. Increased expression of the breast cancer resistance protein (BCRP) in relapsed or refractory acute myeloid leukemia (AML). *Leukemia* **16**:833–839 (2002).
16. J. W. Jonker, G. Merino, S. Musters, A. E. van Herwaarden, E. Bolscher, E. Wagenaar, E. Mesman, T. C. Dale, and A. H. Schinkel. The breast cancer resistance protein BCRP (ABCG2) concentrates drugs and carcinogenic xenotoxins into milk. *Nat. Med.* **11**:127–129 (2005).
17. Y. Imai, M. Nakane, K. Kage, S. Tsukahara, E. Ishikawa, T. Tsuruo, Y. Miki, and Y. Sugimoto. C421A polymorphism in the human breast cancer resistance protein gene is associated with low expression of Q141K protein and low-level drug resistance. *Mol. Cancer Ther.* **1**:611–616 (2002).
18. A. Sparreboom, H. Gelderblom, S. Marsh, R. Ahluwalia, R. Obach, P. Principe, C. Twelves, J. Verweij, and H. L. Mcleod. Diflomotecan pharmacokinetics in relation to ABCG2 421C>A genotype. *Clin. Pharmacol. Ther.* **76**:38–44 (2004).
19. W. Zhang, B. N. Yu, Y. J. He, L. Fan, Q. Li, Z. Q. Liu, A. Wang, Y. L. Liu, Z. R. Tan, Fen-Jiang, Y. F. Huang, and H. H. Zhou. Role of BCRP 421C>A polymorphism on rosuvastatin pharmacokinetics in healthy Chinese males. *Clin. Chim. Acta* **373**:99–103 (2006).
20. Y. Sugimoto, S. Tsukahara, S. Sato, M. Suzuki, H. Nunoi, H. L. Malech, M. M. Gottesman, and T. Tsuruo. Drug-selected co-expression of P-glycoprotein and gp91 *in vivo* from an MDR1-bicistronic retrovirus vector Ha-MDR-IRES-gp91. *J. Gene Med.* **5**:366–376 (2003).
21. Y. Sugimoto, I. Aksentijevich, M. M. Gottesman, and I. Pastan. Efficient expression of drug-selectable genes in retroviral vectors under control of an internal ribosome entry site. *Biotechnology (N Y)* **12**:694–698 (1994).
22. Y. Sugimoto, C. A. Hrycyna, I. I. Aksentijevich, I. I. Pastan, and M. M. Gottesman. Coexpression of a multidrug-resistance gene (MDR1) and herpes simplex virus thymidine kinase gene as part of a bicistronic messenger RNA in a retrovirus vector allows selective killing of MDR1-transduced cells. *Clin. Cancer Res.* **1**:447–457 (1995).
23. Y. Sugimoto, S. Sato, S. Tsukahara, M. Suzuki, E. Okochi, M. M. Gottesman, I. Pastan, and T. Tsuruo. Coexpression of a multidrug resistance gene (MDR1) and herpes simplex virus thymidine kinase gene in a bicistronic retroviral vector Ha-MDR-IRES-TK allows selective killing of MDR1-transduced human tumors transplanted in nude mice. *Cancer Gene Ther.* **4**:51–58 (1997).
24. Z. S. Chen, R. W. Robey, M. G. Belinsky, I. Shchaveleva, X. Q. Ren, Y. Sugimoto, D. D. Ross, S. E. Bates, and G. D. Kruh. Transport of methotrexate, methotrexate polyglutamates, and 17beta-estradiol 17-(beta-D-glucuronide) by ABCG2: effects of acquired mutations at R482 on methotrexate transport. *Cancer Res.* **63**:4048–4054 (2003).
25. E. L. Volk, K. M. Farley, Y. Wu, F. Li, R. W. Robey, and E. Schneider. Overexpression of wild-type breast cancer resistance protein mediates methotrexate resistance. *Cancer Res.* **62**: 5035–5040 (2002).
26. L. F. Payen, M. Gao, C. J. Westlake, S. P. Cole, and R. G. Deeley. Role of carboxylate residues adjacent to the conserved core Walker B motifs in the catalytic cycle of multidrug resistance protein 1 (ABCC1). *J. Biol. Chem.* **278**:38537–38547 (2003).
27. K. Mutoh, J. Mitsuhashi, Y. Kimura, S. Tsukahara, E. Ishikawa, K. Sai, S. Ozawa, J. Sawada, K. Ueda, K. Katayama, and Y. Sugimoto. A T3587G germ-line mutation of the MDR1 gene encodes a nonfunctional P-glycoprotein. *Mol. Cancer Ther.* **5**:877–884 (2006).
28. M. Wada, S. Toh, K. Taniguchi, T. Nakamura, T. Uchiumi, K. Kohno, I. Yoshida, A. Kimura, S. Sakisaka, Y. Adachi, and M. Kuwano. Mutations in the canilicular multispecific organic anion transporter (cMOAT) gene, a novel ABC transporter, in patients with hyperbilirubinemia II/Dubin-Johnson syndrome. *Hum. Mol. Genet.* **7**:203–207 (1998).
29. K. Hashimoto, T. Uchiumi, T. Konno, T. Ebihara, T. Nakamura, M. Wada, S. Sakisaka, F. Maniwa, T. Amachi, K. Ueda, and M. Kuwano. Trafficking and functional defects by mutations of the ATP-binding domains in MRP2 in patients with Dubin-Johnson syndrome. *Hepatology* **36**:1236–1245 (2002).
30. V. Keitel, J. Kartenbeck, A. T. Nies, H. Spring, M. Brom, and D. Keppler. Impaired protein maturation of the conjugate export pump multidrug resistance protein 2 as a consequence of a deletion mutation in Dubin-Johnson syndrome. *Hepatology* **32**:1317–1328 (2000).
31. M. Miwa, S. Tsukahara, E. Ishikawa, S. Asada, Y. Imai, and Y. Sugimoto. Single amino acid substitutions in the transmembrane domains of breast cancer resistance protein (BCRP) alter cross resistance patterns in transfectants. *Int. J. Cancer* **107**:757–763 (2003).
32. S. Mizuarai, N. Aozasa, and H. Kotani. Single nucleotide polymorphisms result in impaired membrane localization and reduced atpase activity in multidrug transporter ABCG2. *Int. J. Cancer* **109**:238–246 (2004).
33. C. P. Zamber, J. K. Lamba, K. Yasuda, J. Farnum, K. Thummel, J. D. Schuetz, and E. G. Schuetz. Natural allelic variants of breast cancer resistance protein (BCRP) and their relationship to BCRP expression in human intestine. *Pharmacogenetics* **13**:19–28 (2003).
34. M. Itoda, Y. Saito, K. Shirao, H. Minami, A. Ohtsu, T. Yoshida, N. Saijo, H. Suzuki, Y. Sugiyama, S. Ozawa, and J. Sawada. Eight novel single nucleotide polymorphisms in ABCG2/BCRP in Japanese cancer patients administered irinotacan. *Drug Metab. Pharmacokinet.* **18**:212–217 (2003).
35. Y. Honjo, K. Morisaki, L. M. Huff, R. W. Robey, J. Hung, M. Dean, and S. E. Bates. Single-nucleotide polymorphism (SNP) analysis in the ABC half-transporter ABCG2 (MXR/BCRP/ABCP1). *Cancer Biol. Ther.* **1**:696–702 (2002).

Inhibition of the mitogen-activated protein kinase pathway results in the down-regulation of P-glycoprotein

Kazuhiro Katayama,[1] Sho Yoshioka,[1] Satomi Tsukahara,[2] Junko Mitsuhashi,[1] and Yoshikazu Sugimoto[1,2]

[1]Department of Chemotherapy, Kyoritsu University of Pharmacy and [2]Division of Gene Therapy, Cancer Chemotherapy Center, Japanese Foundation for Cancer Research, Tokyo, Japan

Abstract

The *multidrug resistance gene 1* (*MDR1*) product, P-glycoprotein (P-gp), pumps out a variety of anticancer agents from the cell, including anthracyclines, *Vinca* alkaloids, and taxanes. The expression of P-gp therefore confers resistance to these anticancer agents. In our present study, we found that FTI-277 (a farnesyltransferase inhibitor), U0126 [an inhibitor of mitogen-activated protein kinase/extracellular signal-regulated kinase (ERK) kinase (MEK)], and 17-allylamino-17-demethoxygeldanamycin (an inhibitor of heat shock protein 90) reduced the endogenous expression levels of P-gp in the human colorectal cancer cells, HCT-15 and SW620-14. In contrast, inhibitors of phosphatidylinositol 3-OH kinase, mammalian target of rapamycin, p38 mitogen-activated protein kinase, and c-Jun NH_2-terminal kinase did not affect P-gp expression in these cells. We further found that U0126 down-regulated exogenous P-gp expression in the *MDR1*-transduced human breast cancer cells, MCF-7/MDR and MDA-MB-231/MDR. However, the *MDR1* mRNA levels in these cells were unaffected by this treatment. PD98059 (a MEK inhibitor), *ERK* small interfering RNA, and *p90 ribosomal S6 kinase* (*RSK*) small interfering RNA also suppressed P-gp expression. Conversely, epidermal growth factor and basic fibroblast growth factor enhanced P-gp expression, but the *MDR1* mRNA levels were unchanged in epidermal growth factor–stimulated cells. Pulse-chase analysis revealed that U0126 promoted P-gp degradation but did not affect the biosynthesis of this gene product. The pretreatment of cells with U0126 enhanced the paclitaxel-induced cleavage of poly(ADP-ribose) polymerase and paclitaxel sensitivity. Furthermore, U0126-treated cells showed high levels of rhodamine123 uptake. Hence, our present data show that inhibition of the MEK-ERK-RSK pathway down-regulates P-gp expression levels and diminishes the cellular multidrug resistance. [Mol Cancer Ther 2007;6(7):2092–2102]

Introduction

The acquisition of multidrug resistance to anticancer agents by tumor cells is characterized by a cross-resistance to structurally unrelated agents (1). Such multidrug-resistant cells express ATP-binding cassette (ABC) transporters, such as P-glycoprotein (P-gp)/ABCB1, breast cancer resistance protein (BCRP)/ABCG2, and multidrug resistance-related protein 1/ABCC1. These gene products pump out a variety of anticancer agents from the cell in energy-dependent manners. Human P-gp is a 170 to 180 kDa plasma membrane glycoprotein encoded by *multidrug resistance gene 1* (*MDR1*), and contains two ATP-binding sites and two transmembrane domains. P-gp functions as an efflux pump for different anticancer agents such as anthracyclines, *Vinca* alkaloids, and taxanes (1–4). Thus, P-gp–expressing cells display low intracellular concentrations of these agents and are resistant to their cytotoxic effects. P-gp is widely expressed in human tissues, including the adrenal gland, colon, kidney, liver, angioendothelial cells, and hematopoietic precursor cells (5–7), and its expression has been shown to be significantly elevated in drug-resistant tumors of the colon, kidney, and liver (8). P-gp expression levels have also been reported to be augmented in some cancers following a recurrence after chemotherapy (8). Hence, the P-gp expression status can significantly affect the sensitivity of cancer cells to its substrate anticancer agents.

The mitogen-activated protein kinase (MAPK) pathways are activated by various kinds of stimuli, including those provided by growth factors, different types of stress, or inflammatory cytokines, and this can result in cell proliferation, differentiation, development, inflammation, or apoptosis (9). The principal components of the MAPK comprise three subfamilies: extracellular signal-regulated kinase (ERK) 1/2, c-Jun NH_2-terminal kinase (JNK)/stress-activated protein kinase (SAPK), and p38MAPK. The activities of the MAPKs are regulated by two events, phosphorylation and dephosphorylation. The MAPK-associated pathways are composed of a growth factor–responsive pathway, including ERK1/2, and two stress-responsive pathways, including JNK/SAPK and p38MAPK. The former comprises Ras, Raf-1, MAPK/ERK kinase (MEK) 1/2, ERK1/2, and p90 ribosomal S6 kinase (RSK) 1/2/3/4. In cells stimulated by growth factors [e.g., epidermal growth factor (EGF) and basic fibroblast growth factor (bFGF)], the Ras proto-oncogene is activated

Received 3/5/07; accepted 5/30/07.

Grant support: The Ministry of Education, Culture, Sports, Science, and Technology, and the Ministry of Health, Labor and Welfare, Japan.

The costs of publication of this article were defrayed in part by the payment of page charges. This article must therefore be hereby marked *advertisement* in accordance with 18 U.S.C. Section 1734 solely to indicate this fact.

Requests for reprints: Yoshikazu Sugimoto, Department of Chemotherapy, Kyoritsu University of Pharmacy, 1-5-30 Shibakoen, Minato-ku, Tokyo 105-8512, Japan. Phone: 81-3-5400-2670; Fax: 81-3-5400-2669. E-mail: sugimoto-ys@kyoritsu-ph.ac.jp

doi:10.1158/1535-7163.MCT-07-0148

via receptor protein tyrosine kinases such as EGF receptor (EGFR) and FGF receptor. Ras can associate with the plasma membrane by virtue of lipid modifications at its COOH terminus (10). This recruitment to the plasma membrane transduces Ras from an inactive form (GDP-Ras) to an active form (GTP-Ras), and is essential for activation by growth factors (10). GTP-Ras interacts with Raf-1, localizing the latter to the plasma membrane where it becomes activated by several kinases and phosphatases (9). Activated Raf-1 then induces the sequential activation of MEK1/2 and ERK1/2 in a phosphorylation-dependent manner. Activated ERK1/2 then translocate from the cytoplasm to the nucleus and activate a number of transcription factors associated with cell cycle progression, survival, development, and differentiation (9). ERK1/2 also transduce signals to RSKs and thereby positively regulate cell cycle progression by promoting the cyclic AMP response element binding protein–dependent transactivation of cyclin A and cyclin D1, and by inhibiting the nuclear translocation of the cyclin-dependent kinase inhibitor, $p27^{Kip1}$ (11–13). Hence, the MEK-ERK-RSK pathway plays a central role during cell growth and survival.

In our previous studies, we have shown that estrogens down-regulate both P-gp and BCRP expression levels (14, 15). We have also further shown that the down-regulation of BCRP by 17β-estradiol (E_2) is dependent on the posttranscriptional inhibition of protein biosynthesis, but not on protein degradation (14). It has been shown by others that phosphatidylinositol 3-OH kinase (PI3K) inhibitors also down-regulate BCRP expression levels (16). Studies of small molecules or physiologic compounds that suppress ABC transporter protein expression are thus now ongoing. In our present study, we examine the effects of several signal transduction inhibitors upon the expression levels of P-gp, and find that U0126, PD98059, *ERK* small interfering RNA (siRNA), and *RSK* siRNA inhibit P-gp expression. Moreover, U0126 down-regulate P-gp expression by promoting its degradation, but does not affect its biosynthesis. Our present findings thus provide an increased understanding of P-gp biosynthesis and degradation and reveal potential new strategies for the circumvention of P-gp–mediated drug resistance.

Materials and Methods

Reagents

U0126 and PD98059 were purchased from Cell Signaling Technology. 17-Allylamino-17-demethoxygeldanamycin (17-AAG) was purchased from Alomone Labs. Rapamycin, SP600125, EGF, bFGF, and rhodamine123 were purchased from Sigma. FTI-277, LY294002, and SB203580 were obtained from Calbiochem. Paclitaxel was obtained from Bristol-Myers Squibb.

Antibodies for Western blotting were purchased as follows: anti-MDR1+3 monoclonal antibody (C219; Zymed); anti-glyceraldehyde-3-phosphate dehydrogenase (GAPDH) monoclonal antibody (Chemicon); anti-p44/p42, anti–phospho-p44/p42 (Thr^{202}/Tyr^{204}), anti-Akt, and anti–phospho-Akt (Ser^{473}) polyclonal antibodies and anti–phospho-EGFR (Tyr^{1068}) monoclonal antibody (Cell Signaling Technology); anti-EGFR monoclonal antibody (Santa Cruz Biotechnology); and anti–poly(ADP-ribose) polymerase (PARP) p85 fragment polyclonal antibody (Promega).

Cells

The human cancer cell lines used in this study were obtained from the National Cancer Institute (Bethesda, MD). SW620-14 cells were isolated from human colorectal tumor SW620 cells by limiting dilution. The *MDR1*-transduced human breast cancer cell lines MCF-7/MDR and MDA-MB-231/MDR were established by transduction with the HaMDR retrovirus as described previously (15). MDA-MB-231 cells were transduced with the Ha3HisMDR retrovirus harboring 3′-His–tagged human *MDR1* cDNA. The transduced cells were selected with 3 nmol/L vincristine for 10 days and the resulting mixed population was designated MDA-MB-231/3HisMDR. All cells were cultured in the growth medium consisting of 93% DMEM and 7% fetal bovine serum (FBS) at 37°C in 5% CO_2.

Western Blotting and Immunoprecipitation

Cell membrane and cytoplasmic fractions were prepared from cells in lysis buffer [0.2% NP40, 10% glycerol, 137 mmol/L NaCl, 20 mmol/L Tris-Cl (pH 7.5), 1.5 mol/L $MgCl_2$, 1 mmol/L EDTA (pH 8.0), 50 mmol/L NaF, 1 mmol/L Na_3PO_4, 12 mmol/L β-glycerophosphate, 1 mmol/L phenylmethylsulfonyl fluoride, 1 mmol/L aprotinin]. For immunoprecipitation of 3HisP-gp from MDA-MB-231/3HisMDR cells, 500 μg of protein were incubated with Ni-NTA agarose (Qiagen) for 2 h on ice with occasional tapping. The immunocomplexes precipitated with the Ni-NTA agarose were then washed five times with ice-cold wash buffer [1 mol/L Tris-Cl (pH 7.5), 1 mol/L NaCl, 1% Triton X-100]. Whole-cell lysates were prepared with SDS-containing lysis buffer [1% SDS, 10% glycerol, and 100 mmol/L Tris-Cl (pH 7.5)]. All cell lysates and immunoprecipitates were solubilized with sample buffer [2% SDS, 50 mmol/L Tris-HCl (pH 8.0), 0.2% bromophenol blue, 5% 2-mercaptoethanol] with boiling for 5 min at 100°C, separated by SDS-PAGE, and then transferred onto nitrocellulose membranes. The membranes were incubated with primary antibodies following by peroxidase-conjugated sheep anti-mouse or anti-rabbit secondary antibodies (Amersham Biosciences Corp.). Bands were visualized with the ECL (enhanced chemiluminescence) Plus detection kit (Amersham Biosciences Corp.).

siRNA Transfection

Nonsilencing control siRNA were purchased from Qiagen. *ERK* siRNA was obtained from Cell Signaling Technology and comprises a mixture of *ERK1* and *ERK2* siRNAs. *RSK* siRNA was purchased from Qiagen and was composed of *RSK1*, *RSK2*, and *RSK3* siRNAs. Cells were transfected with these siRNAs using Lipofectamine 2000 (Invitrogen), according to the manufacturer's instructions.

Plasmid DNAs and Transfection

Human wild-type (WT) *H-Ras, Raf-1, MEK1, MEK2, ERK1, ERK2, RSK1, RSK2, p85α* regulatory subunit of *PI3K, akt1*, and *phosphatase and tensin homologue deleted in chromosome 10* (*PTEN*) cDNAs were generated by PCR with a Human Liver BD Marathon-Ready cDNA (BD Biosciences Clontech) as the template. The PCR products were then digested and cloned into the pFLAG-CMV-2 vector (Sigma). Mutant *PTEN* cDNA was constructed by the substitution of Cys^{124} with Ser of *PTEN* (WT) using a QuickChange Site-Directed Mutagenesis kit (Stratagene). Cells were transfected with these plasmid DNAs using LipofectAMINE 2000 (Invitrogen).

Semiquantitative Reverse Transcription-PCR of *MDR1*

Cells were treated with either 10 μmol/L U0126 or 100 μg/L EGF, and total RNA was then extracted using an RNeasy kit (Qiagen). Reverse transcription-PCR (RT-PCR) was done using RNA LA PCR kit (Takara) as described previously (15). Real-time RT-PCR was done using SYBR Green PCR Master Mix and RT-PCR Reagents (Applied Biosystems) and an ABI PRISM 7700 Sequence Detection System (Applied Biosystems).

Fluorescence-Activated Cell Sorting Analysis

The expression levels of P-gp on the cell surface after treatment with 10 μmol/L U0126 for 72 h were detected by fluorescence-activated cell sorting analysis using a human-specific monoclonal antibody, MRK16, raised against P-gp. Cells were incubated with or without a biotinylated $F(ab')_2$ fragment of MRK16 (100 μg/mL). The cells were then washed and incubated with R-phycoerythrin–conjugated streptavidin (400 μg/mL; Becton Dickinson and Company). Fluorescence staining levels were detected using FACSCalibur (Becton Dickinson and Company).

The cellular accumulation of rhodamine123, a substrate of P-gp, was determined by flow cytometry. Cells were treated with 10 μmol/L U0126 for 72 h, and the medium was changed every 24 h. After trypsinization, the cells (1×10^5) were washed with ice-cold PBS, resuspended in 1 mL of DMEM supplemented with 300 nmol/L rhodamine123, and incubated for 20 min at 37°C. The cells were then washed twice with ice-cold PBS, and the intracellular accumulation of rhodamine123 was measured using FACSCalibur.

Metabolic Labeling of P-gp in MDA-MB-231/3HisMDR Cells

To examine the biosynthesis profile of P-gp, MDA-MB-231/3HisMDR cells (1×10^6 cells/25 cm^2 flask) were incubated in methionine- and cysteine-free DMEM (Invitrogen) supplemented with 7% dialyzed charcoal/dextran-treated FBS (HyClone; labeling medium) for 1.5 h just before the beginning of the experiments. The cells were then incubated in the labeling medium containing 300 μCi/mL of [^{35}S]methionine/cysteine for either 0.5 or 1 h. For U0126-treated cells, 10 μmol/L U0126 was added at 4 h before the start of the experiment. Cells were then harvested and lysed with lysis buffer. 3HisP-gp was immunoprecipitated with Ni-NTA agarose and solubilized with 2× sample buffer as described above. The labeled protein was then subjected to SDS-PAGE and autoradiographed. The band intensities of the labeled P-gp were quantified using the NIH-Image densitometric program. Each column represents the mean ± SD from three independent experiments.

To examine the degradation of P-gp, MDA-MB-231/3HisMDR cells (1×10^6 cells/25 cm^2 flask) were incubated in the labeling medium for 1.5 h just before starting the experiment and then incubated in the labeling medium containing 300 μCi/mL of [^{35}S]methionine/cysteine for 1 h. The labeling medium was then replaced with the growth medium, and the cells were chased for 2 to 12 h. For U0126-treated cells, 10 μmol/L U0126 was added to the medium throughout the experiment. The band intensities of the labeled P-gp were again quantified using NIH Image and calculated as a percentage of the control (labeled sample with no chase; 0 h).

Results

The Inhibitors of MEK-ERK-RSK Pathway Suppress P-gp Expression

The human colorectal tumor cell lines HCT-15 and SW620-14, which both express endogenous P-gp, were treated with either 10 μmol/L FTI-277 (an inhibitor of farnesyltransferase that activates Ras), 10 μmol/L U0126 (a MEK1/2 inhibitor), 100 nmol/L 17-AAG (an inhibitor of heat shock protein 90 that stabilizes both Raf-1 and PDK1), 50 μmol/L LY294002 (a PI3K inhibitor), or 100 nmol/L rapamycin [an inhibitor of mammalian target of rapamycin (mTOR)] for 12 h. The P-gp expression levels were then determined by Western blot analysis. As shown in Fig. 1A, the cells treated with FTI-277, U0126, and 17-AAG showed 5- to 20-fold lower levels of P-gp compared with untreated cells. However, neither LY294002 nor rapamycin treatments affected P-gp expression. To exclude the possibility that the down-regulation of P-gp in these analyses was due to an alteration in the status and solubility of the protein in 0.2% NP40, we also analyzed its expression using whole cell lysates. In this experiment, U0126 and 17-AAG again suppressed P-gp expression in HCT-15 and SW620-14 cells (Fig. 1B). We next examined whether either SB203580 (a p38MAPK inhibitor) or SP600125 (a JNK inhibitor) affected P-gp expression levels in HCT-15 and SW620-14 cells. However, upon treatment with 10 μmol/L SB203580 or 20 μmol/L SP600125 for 12 h, the P-gp expression levels were found to be unchanged in these cells (Fig. 1C).

MEK Inhibitors Down-regulate P-gp Expression in a Time-Dependent Manner

We next examined the suppressive effects of U0126 in exogenous P-gp–expressing cells. We also examined the time dependency of the down-regulation of P-gp by U0126. HCT-15, SW620-14, MCF-7/MDR, and MDA-MB-231/MDR cells were treated with 10 μmol/L U0126 for 2 to 16 h, and P-gp expression levels were determined by Western blotting. U0126 was found to down-regulate exogenous P-gp expression also in these *MDR1*-transduced cell lines

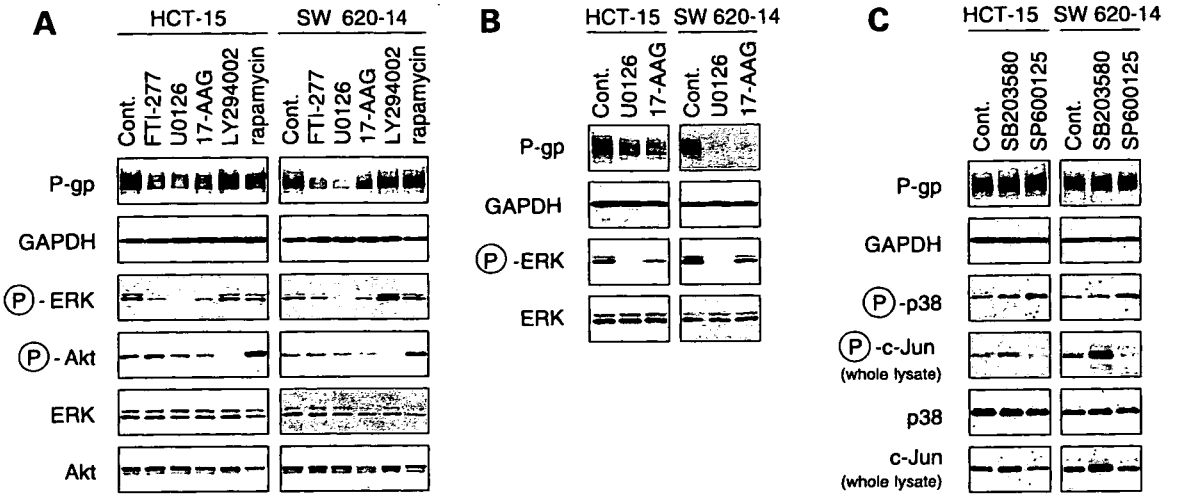

Figure 1. Screening of the effects of various kinase inhibitors upon P-gp expression levels. **A,** Western blot analysis of endogenous P-gp expression levels in both cell membrane and cytoplasmic fractions of cells treated with inhibitors against the MEK-ERK-RSK or PI3K-Akt-mTOR pathway. HCT-15 or SW620-14 cells were treated with either medium alone (*Cont.*), 10 μmol/L FTI-277, 10 μmol/L U0126, 100 nmol/L 17-AAG, 20 μmol/L LY294002, or 10 μmol/L rapamycin for 12 h. Cellular membrane and cytoplasmic fractions were prepared with lysis buffer containing 0.2% NP40 and subjected to Western blotting with the indicated antibodies. **B,** Western blot analysis of P-gp expression levels in whole-cell lysates of U0126- or 17-AAG – treated cells. HCT-15 or SW620-14 cells were treated with either medium alone, 10 μmol/L U0126, or 100 nmol/L 17-AAG. After 12 h, whole-cell lysates were obtained using lysis buffer containing 1% SDS and subjected to Western blotting with the indicated antibodies. **C,** Western blot analysis of P-gp expression levels in cells treated with p38MAPK or JNK inhibitor. HCT-15 or SW620-14 cells were treated with either medium alone, 10 μmol/L SB203580, or 20 μmol/L SP600125 for 12 h. Cells were harvested and divided into two groups. One was lysed with lysis buffer containing 1% SDS to analyze the expression levels of total c-Jun and phosphorylated c-Jun, and another was lysed with lysis buffer containing 0.2% NP40 to analyze the other indicated proteins. The lysates were then subjected to Western blotting with the indicated antibodies.

(Fig. 2A). The time dependency of this suppression varied among the cell lines, as it was evident within 4 h in SW620-14 cells, but required 8 h in HCT-15 and MCF-7/MDR cells and 12 h in MDA-MB-231/MDR cells. As a control experiment, we examined the time dependency of P-gp expression in the absence of the inhibitor. The same cells were cultured for a further 2 to 16 h after changing the medium to the flesh growth medium without inhibitors, and the P-gp levels were found to be unchanged at each time point for each cell line (Fig. 2B).

We next examined *MDR1* mRNA expression levels by RT-PCR. Each of the HCT-15, SW620-14, MCF-7/MDR, and MDA-MB-231/MDR cells were treated with U0126 under the same conditions used for the experiments in Fig. 2A. Total RNAs were isolated from these cells and RT-PCR was done using *MDR1* or *GAPDH*-specific oligonucleotides. As shown in Fig. 2C, the *MDR1* mRNA levels were unchanged after U0126 treatment at all time points in each of the cell lines. Similar results were obtained using real-time PCR analysis (Supplementary Fig. S1A).[3] P-gp expression levels were then examined in these cells after treatment with another MEK inhibitor, PD98059, at a concentration of 50 μmol/L for 8 or 12 h. Similar to the findings shown in Fig. 2A, all of the cell lines tested in this experiment expressed lower levels of P-gp after PD98059 treatment, compared with untreated cells (Fig. 2D).

We further examined the effects upon P-gp expression when either ERK or RSK was specifically suppressed by siRNA. Each of our four test cell lines was transfected with either a nonsilencing control, *ERK* siRNA, or *RSK* siRNA, and the P-gp expression levels were then determined by Western blotting after 48 h. P-gp was found to be down-regulated by the knockdown of both the ERK and RSK proteins in a dose-dependent manner (Fig. 2E). The suppression of RSK in particular had a significant negative effect upon P-gp expression (Fig. 2E). Fluorescence-activated cell sorting analysis also revealed that cells treated with U0126 for 72 h expressed lower amounts of cell surface P-gp compared with untreated cells (Fig. 3). From these data, we conclude that P-gp expression is suppressed by a blockade of the MEK-ERK-RSK pathway.

EGF or bFGF Stimulation Enhances P-gp Expression but Does Not Affect *MDR1* Transcription

Given that the inhibition of the MEK-ERK-RSK pathway suppressed P-gp expression, we next investigated whether the activation of this pathway would in fact enhance P-gp. HCT-15, SW620-14, MCF-7/MDR, and MDA-MB-231/MDR cells were cultured in serum-free DMEM for 6 h and incubated in the growth medium supplemented with 100 μg/L EGF for a further 2 to 16 h. Western blot analysis revealed that EGF activated EGFR (increased levels of phosphorylated EGFR are detectable), and that upon induction of the MEK-ERK-RSK pathway (increased phosphorylation of ERK) there was an observable increase in the P-gp expression levels in all cells (Fig. 4A). To examine the effects of serum starvation itself on P-gp

[3] Supplementary material for this article is available at Molecular Cancer Therapeutics Online (http://mct.aacrjournals.org/).